GLOBAL BIOGEOCHEMICAL CYCLES, VOL. 15, NO. 4, PAGES 845–862, DECEMBER 2001

Basin-wide particulate carbon flux in the Atlantic Ocean: Regional export patterns and potential for atmospheric CO_2 sequestration

Avan N. Antia,[1] Wolfgang Koeve,[1,2] Gerhard Fischer,[3] Thomas Blanz,[1,4] Detlef Schulz-Bull,[1,4] Jan Scholten,[5] Susanne Neuer,[6] Klaus Kremling,[1] Joachim Kuss,[1,4] Rolf Peinert,[1] Dirk Hebbeln,[3] Ulrich Bathmann,[7] Maureen Conte,[8] Uwe Fehner,[1] and B. Zeitzschel[1]

Abstract. Particle flux data from 27 sites in the Atlantic Ocean have been compiled in order to determine regional variations in the strength and efficiency of the biological pump and to quantify carbon fluxes over the ocean basin, thus estimating the potential oceanic sequestration of atmospheric CO_2. An algorithm is derived relating annual particulate organic carbon (POC) flux to primary production and depth that yields variations in the export ratio (ER = POC flux/primary production) at 125 m of between 0.08 and 0.38 over the range of production from 50 to 400 g C m^{-2} yr^{-1}. Significant regional differences in changes of the export ratio with depth are related to the temporal stability of flux. Sites with more pulsed export have higher export ratios at 125 m but show more rapid decreases of POC flux with depth, resulting in little geographic variation in fluxes below ~3000 m. The opposing effects of organic carbon production and calcification on ΔpCO_2 of surface seawater are considered to calculate an "effective carbon flux" at the depth of the euphotic zone and at the base of the winter mixed layer. POC flux at the base of the euphotic zone integrated over the Atlantic Ocean between 65°N and 65°S amounts to 3.14 Gt C yr^{-1}. Of this, 5.7% is remineralized above the winter mixed layer and thus does not contribute to CO_2 sequestration on climatically relevant timescales. The effective carbon flux, termed J_{eff}, amounts to 2.47 Gt C yr^{-1} and is a measure of the potential sequestration of atmospheric CO_2 for the area considered. A shift in the composition of sedimenting particles (seen in a decrease of the opal:carbonate ratio) is seen across the entire North Atlantic, indicating a basin-wide phenomenon that may be related to large-scale changes in climatic forcing.

1. Introduction

Publications dealing with carbon flux in the ocean often introduce the issue in terms of the biological pump, drawing down (anthropogenic) CO_2 from the atmosphere, with the potential to shape and/or modulate climate. Although in the framework of climatic processes the physical pump dominates in strength, the biological pump (through particle formation and vertical export) is the only process that drives gradients in seawater carbonate chemistry across physical boundaries. Globally, sinking particles transfer ~0.4 Gt C yr^{-1} from the ocean surface to deeper water [*Lampitt and Antia*, 1997; *Schlitzer*, 2000] and to the sediment surface [*Jahnke*, 1996]. Perhaps more importantly, biology responds to changes in climatic conditions in a manner that is complex and can be nonlinear, triggering shifts in functional groups of organisms that change the oceans' biogeochemical functioning [e.g., *Karl et al.*, 1997; *Riebesell et al.*, 2000].

A major goal of the Joint Global Ocean Flux Study (JGOFS) has been to better understand the physical and biological conditions that control regional variations in the strength and efficiency of the biological pump. The net effect of the biological pump on drawdown of atmospheric CO_2 depends on three main characteristics. First, the mode and speed of particle sinking determines the depth to which particles are exported and the degree to which they are remineralized in the water column. Empirical studies have yielded algorithms linking primary production to particulate organic carbon (POC) flux and water depth [e.g., *Suess*, 1980; *Pace et al.*, 1987; *Berger et al.*, 1987] that are useful for calculating the fraction of productivity that is exported (i.e., the export ratio, ER = POC flux/primary production). There are significant regional differences in the ER normalized to a single depth (e.g., ER_{2000m} by *Lampitt and Antia* [1997] and ER_{1000m} by *Fischer et al.* [2000]). However, little is known about regional and temporal variations in the rate of decrease of POC flux with depth. This will be determined by the mode of export and the composition of sedimenting particles.

[1]Institut für Meereskunde, Forschungsbereich Biogeochemie, Kiel, Germany.
[2]Also at Laboratoire d'Etudes en Geophysique et Oceanographie Spatiale, Toulouse, France.
[3]Fachbereich Geowissenschaften, Universität Bremen, Bremen, Germany.
[4]Now at Institut für Ostseeforschung-Warnemünde, Warnemünde, Germany.
[5]Geologisches Institut, Universität Kiel, Kiel, Germany.
[6]Department of Biology, Arizona State University, Tempe, Arizona, USA.
[7]Alfred Wegener Institut für Polarforschung, Bremerhaven, Germany.
[8]Woods Hole Oceanographic Institution, Woods Hole, Massachusetts, USA.

Paper number 2000GB001376.
0886-6236/01/2000GB001376$12.00

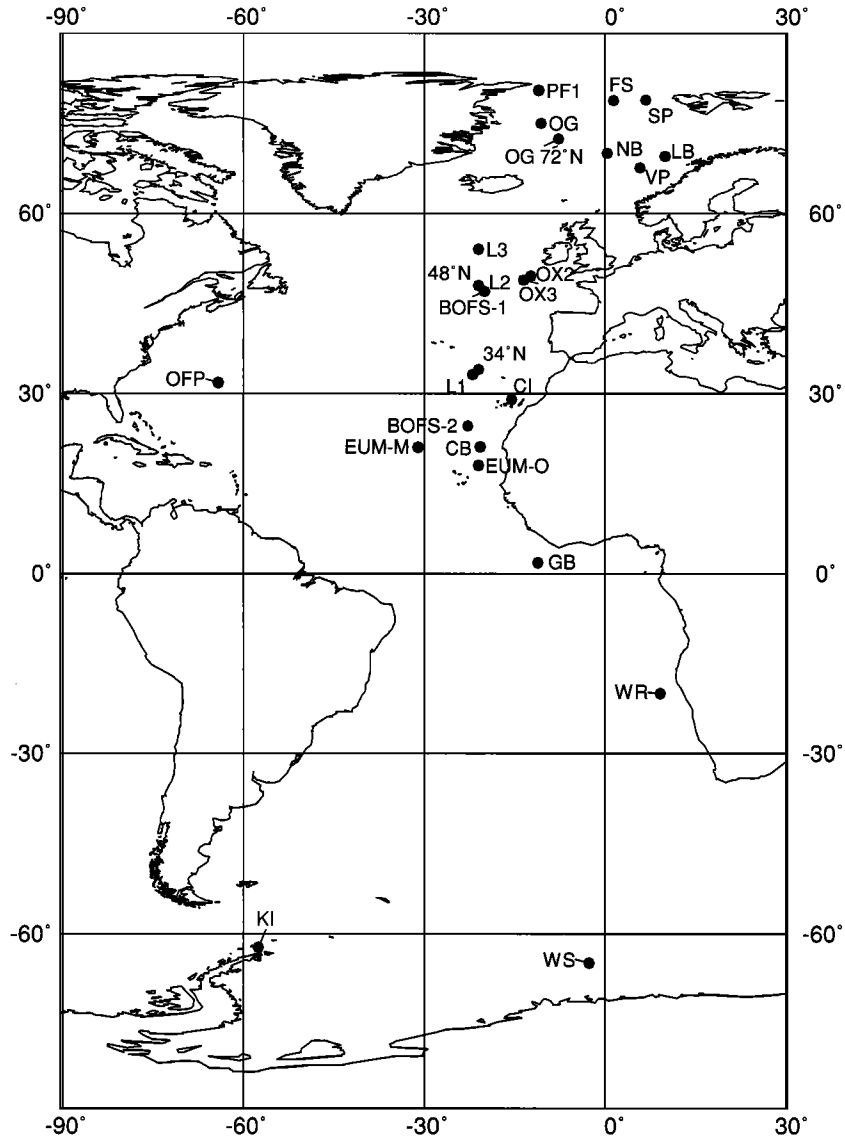

Figure 1. Locations of moorings from which data are used in this study. Station abbreviations are listed in Table 1.

Second, the drawdown of atmospheric CO_2 is not just a function of the organic tissue pump but results from the ratio of particulate organic carbon (POC) to particulate inorganic carbon (PIC = calcite + aragonite) in export, termed the rain ratio (RR = POC:PIC), since photosynthesis and calcification have opposing effects on seawater pCO_2 [*Frankignoulle et al.*, 1994; *Archer and Meier-Reimer*, 1994]. The rain ratio is thus a measure of the "efficiency" of biological carbon sequestration. The carbonate (alkalinity) pump changes the total carbon:total nitrogen ratio of export (and thus has an effect on ΔpCO_2 between the atmosphere and surface ocean) that is decoupled from the ratio of carbon to nitrogen in subthermocline upwelled water. Globally, there are large variations in the rain ratio (POC:PIC) in sedimenting particles, with higher ratios in the Pacific Ocean than in the Atlantic Ocean and higher rain ratios in polar regions and at continental margins than in the nonpolar open ocean [*Tsunogai and Noriki*, 1991].

Third, it is important to emphasize that for carbon export to be effective on climatically relevant timescales, particles must leave the seasonally mixed layer, that is, that layer which is mixed at least once during winter overturning. The widely used concept of new production and export production [*Dugdale and Goering*, 1967; *Eppley and Peterson*, 1979] equates the sum of allochthonous nitrogen inputs into the euphotic zone through vertical mixing, nitrogen fixation, and other external sources with the downward fluxes of particulate organic nitrogen (PON) and dissolved organic nitrogen (DON). Since DON fluxes at the base of the euphotic zone may not be negligible, particulate organic matter flux can approximate but probably never equal new production. Equating new production to export production and using global and regional estimates of new production [*Falkowski et al.*, 1998; *Oschlies and Garcon*, 1998] thus allows estimation of the fraction of primary production available to export in organic particles. New production does not, however, quantify carbon export in any climatically relevant sense since (1) the CO_2 released during respiration (or taken up during calcite dissolution) equilibrates with the atmosphere to the depth of maximal seasonal ventilation and not the euphotic depth and (2) the net effect of biology on seawater pCO_2 must include calcite formation and export, which is decoupled from new production. Highest POC remineralization [e.g., *Suess*, 1980] and calcite dissolution [*Milliman et al.*, 1999] rates occur between the euphotic zone and the winter mixed layer (WML)

Table 1. Mooring Sites, Bulk Fluxes, Trap Collection Efficiencies and Data Sources of Data Used in This Study[a]

Mooring Site	ID	Water Depth, m	Trap Depth, m	Latitude °N	Longitude °W	Date		Interval, days	Total Mass, g m^{-2} yr^{-1}	POC, g m^{-2} yr^{-1}	Trap Efficiency,[b] %	Source
						Start	End					
NE Polynya	PF1	295	130	80.5	11.0	Aug. 2, 1992	Aug. 2, 1993	365	11.19	1.10		*Bauerfeind et al.* [1997]
NE Polynya		335	130	80.4	14.6	Aug. 2, 1992	Aug. 2, 1993	365	4,71	0.42		*Bauerfeind et al.* [1997]
Spitzbergen	SP	1676	1125	78.9	−6.8	Dec. 9, 1988	Dec. 9, 1989	365	183.34	6.66		*Hebbeln* [2000]
Fram Strait	FS	2821	2440	78.8	−1.4	Aug. 19, 1984	Aug. 31, 1985	377	6.70	0.44		*Honjo et al.* [1988]
Fram Strait		2487	1488	78.8	−0.2	July 1, 1987	June 15, 1988	350	60.40	3.06		*Hebbeln and Wefer* [1991]
Fram Strait		1763	1191	78.4	4.1	July 1, 1988	May 29, 1989	332	2.89	0.29		*Hebbeln and Wefer* [1991]
East Greenland Sea (75°N)	OG 75°N	3073	500	75.0	10.6	July 23, 1994	July 23, 1995	365	77.39	4.23		*Peinert et al.* [2001]
East Greenland Sea (75°N)		3073	2000	74.6	10.4	Aug. 10, 1994	Oct. 11, 1995	427	66.54	2.18		*Peinert et al.* [2001]
East Greenland Sea (72°N)	OG 72°N	2624	500	72.4	7.7	Feb. 25, 1991	Feb. 25, 1992	365	10.89	1.69		*von Bodungen et al.* [1995]
East Greenland Sea (72°N)		2240	500	72.1	7.0	Feb. 18, 1989	March 2, 1990	377	24.54	3.69		*von Bodungen et al.* [1995]
East Greenland Sea (72°N)		2631	1000	72.4	7.7	Feb. 25, 1991	Feb. 25, 1992	365	11.20	1.17		*von Bodungen et al.* [1995]
East Greenland Sea (72°N)		2631	2200	72.4	7.7	Feb. 25, 1991	Feb. 25, 1992	365	11.67	0.55		*von Bodungen et al.* [1995]
Norwegian Basin	NB	3350	500	70.0	−0.4	Feb. 19, 1992	Feb. 19, 1993	366	21.01	1.76		*Peinert et al.* [2001]
Norwegian Basin		3350	1000	70.0	−0.4	Feb. 19, 1992	Feb. 19, 1993	366	21.63	2.31		*Peinert et al.* [2001]
Norwegian Basin		3350	3000	70.0	−0.4	Feb. 19, 1992	Feb. 19, 1993	366	48.65	2.24		*Peinert et al.* [2001]
Norwegian Basin		3350	3000	70.0	−0.4	Feb. 20, 1987	Feb. 21, 1988	366	41.54	2.96		*von Bodungen et al.* [1995]
Lofoten Basin	LB	3160	2760	69.5	−10.0	July 31, 1983	July 14, 1984	349	22.00	1.34		*Honjo et al.* [1988]
Voering Plateau	VP	1440	500	67.6	−5.8	March 23, 1987	March 22, 1988	365	30.73	3.46		*von Bodungen et al.* [1995]
German JGOFS-L3	L3	3070	1000	54.0	21.0	July 29, 1995	July 3, 1996	340	27.31	4.43	38	D. Schulz-Bull et al. (unpublished data, 2001)
German JGOFS-L3		3070	1000	54.0	21.0	March 20, 1996	March 22, 1997	367		1.15	38	D. Schulz-Bull et al. (unpublished data, 2001)
German JGOFS-L3		3070	2200	54.0	21.0	March 20, 1994	March 20, 1995	365	18.67	0.57	77	*Kuss and Kremling* [1999]
German JGOFS-L3		3070	2200	54.0	21.0	March 21, 1995	March 22, 1996	367	22.77	2.13	77	D. Schulz-Bull et al. (unpublished data, 2001)
German JGOFS-L3		3070	2200	54.0	21.0	March 20, 1996	March 22, 1997	367	15.34	0.65	77	D. Schulz-Bull et al. (unpublished data, 2001)
OMEX 2	OX2	1500	600	49.6	12.3	July 1, 1993	July 1, 1994	365	18.95	2.10	38	*Antia et al.* [1999]
OMEX 2		1500	1050	49.6	12.3	July 1, 1993	July 1, 1994	365	26.48	2.22		*Antia et al.* [1999]
OMEX 3	OX3	3260	580	48.9	13.5	July 1, 1993	May 20, 1994	323	12.00	1.78	34	*Antia et al.* [1999]
OMEX 3		3260	1440	48.9	13.5	July 1, 1993	July 1, 1994	365	42.50	3.61		*Antia et al.* [1999]
OMEX 3		3260	3220	48.9	13.5	July 1, 1993	July 1, 1994	365	37.78	1.89		*Antia et al.* [1999]
Honjo-48°N	48°N	4435	1000	48.0	21.0	April 3, 1989	April 2, 1990	364	20.70	1.48	41	*Honjo and Manganini* [1993]
Honjo-48°N		4435	1000	48.0	21.0	April 3, 1989	April 2, 1990	364	26.90	1.38		*Honjo and Manganini* [1993]
Honjo-48°N		4000	3300	48.0	21.0	April 3, 1989	April 2, 1990	364	26.20	1.00	103	*Honjo and Manganini* [1993]
BOFS-49°N	BOFS-1	4555	3100	47.0	20.0	April 18, 1989	April 22, 1990	369	22.06	1.78	80	*Newton et al.* [1994]
German JGOFS-L2	L2	4481	500	47.0	20.0	April 4, 1992	April 4, 1993	365	7.57	0.77	15	U. Fehner abd W. Koeve (unpublished data, 2001)
German JGOFS-L2		4481	500	47.0	20.0	March 20, 1994	March 23, 1995	368	5.05	0.62	15	U. Fehner abd W. Koeve (unpublished data, 2001)
German JGOFS-L2		4481	1000	47.0	20.0	March 28, 1992	March 28, 1993	365	11.21	1.20	20	*Kuss and Kremling* [1999]
German JGOFS-L2		4481	2000	47.0	20.0	March 20, 1994	March 20, 1995	365	24.37	0.90	54	*Kuss and Kremling* [1999]

Table 1. (continued)

Mooring Site	ID	Water Depth, m	Trap Depth, m	Latitude °N	Longitude °W	Date Start	Date End	Interval, days	Total Mass, g m^{-2} yr^{-1}	POC, g m^{-2} yr^{-1}	Trap Efficiency,[b] %	Source
German JGOFS-L2		4481	2000	47.0	20.0	March 23, 1995	March 24, 1996	367	23.27	1.25	54	D. Schulz-Bull et al. (unpublished data, 2001)
German JGOFS-L2		4481	2000	47.0	20.0	March 17, 1996	March 19, 1997	367	20.11	1.33	54	D. Schulz-Bull et al. (unpublished data, 2001)
German JGOFS-L2		4481	3500	47.0	200	March 28, 1992	March 28, 1993	365	15.34	0.65	64	*Kuss and Kremling* [1999]
Honjo-34°N	34°N	5172	1159	34.0	21.0	April 3, 1989	March 18, 1990	349	19.40	1.00	60	*Honjo and Manganini* [1993]
Honjo-34°N		5172	1981	34.0	21.0	April 3, 1989	March 18, 1990	349	22.40	1.03	90	*Honjo and Manganini* [1993]
Honjo-34°N		5172	4472	34.0	21.0	April 3, 1989	March 18, 1990	349	21.90	0.85	123	*Honjo and Manganini* [1993]
German JGOFS-L1	L1	5275	2000	33.1	22.0	March 12, 1994	March 14, 1995	367	13.34	0.62	52	*Kuss and Kremling* [1999]
German JGOFS-L1		5275	2000	33.1	22.0	March 14, 1995	March 16, 1996	368	15.78	0.70	52	D. Schulz-Bull et al. (unpublished data, 2001)
German JGOFS-L1		5275	2000	33.1	22.0	March 20, 1996	March 23, 1997	368	15.18	0.80	52	D. Schulz-Bull et al. (unpublished data, 2001)
German JGOFS-L1		5275	4000	33.1	22.0	Oct. 18, 1993	Sept. 2, 1994	319	18.41	0.67	71	*Kuss and Kremling* [1999]
Sargasso Sea	OFP	4400	500	31.8	64.2	Nov. 17, 1984	Nov. 18.11. 1985	366	12.83	2.25		Ocean Flux Program Web site[c]
Sargasso Sea		4400	500	31.8	64.2	Nov. 11, 1989	Nov. 14.11. 1990	368	8.76	1.02		Ocean Flux Program Web site[c]
Sargasso Sea		4400	500	31.8	64.2	Dec. 13, 1990	Dec. 3, 1991	355	14.79	1.42		Ocean Flux Program Web site[c]
Sargasso Sea		4400	500	31.8	64.2	Dec. 20, 1991	Dec. 19, 1992	365	16.22	1.89		Ocean Flux Program Web site[c]
Sargasso Sea		4400	1500	31.8	64.2	Nov. 17, 1984	Nov. 18, 1985	366	13.62	1.01		Ocean Flux Program Web site[c]
Sargasso Sea		4400	1500	31.8	64.2	Nov. 11, 1987	Nov. 14, 1988	369	15.00	0.98		Ocean Flux Program Web site[c]
Sargasso Sea		4400	1500	31.8	64.2	Nov. 15, 1988	Nov. 11, 1989	361	10.93	0.74		Ocean Flux Program Web site[c]
Sargasso Sea		4400	1500	31.8	64.2	Nov. 11, 1989	Nov. 14, 1990	368	10.96	0.63		Ocean Flux Program Web site[c]
Sargasso Sea		4400	1500	31.8	64.2	Dec. 26, 1990	Dec. 20, 1991	359	16.18	0.93		Ocean Flux Program Web site[c]
Sargasso Sea		4400	1500	31.8	64.2	Dec. 20, 1991	Dec. 19, 1992	365	13.94	0.96		Ocean Flux Program Web site[c]
Sargasso Sea		4400	3200	32.1	64.2	Dec. 6, 1979	Dec. 10, 1980	370	13.86	0.68		Ocean Flux Program Web site[c]
Sargasso Sea		4400	3200	32.1	64.2	Dec. 10, 1980	Dec. 3, 1981	358	18.23	0.89		Ocean Flux Program Web site[c]
Sargasso Sea		4400	3200	32.1	64.2	Dec. 3, 1981	Dec. 8, 1982	370	18.41	0.92		Ocean Flux Program Web site[c]
Sargasso Sea		4400	3200	32.1	64.2	Jan. 18, 1983	Jan. 18, 1984	365	16.16	0.79		Ocean Flux Program Web site[c]
Sargasso Sea		4400	3200	31.8	64.2	Nov. 17, 1984	Nov. 18, 1985	366	12.15	0.65		Ocean Flux Program Web site[c]
Sargasso Sea		4400	3200	31.8	64.2	Nov. 14, 1986	Nov. 10, 1987	361	13.14	0.54		Ocean Flux Program Web site[c]
Sargasso Sea		4400	3200	31.8	64.2	Nov. 11, 1987	Nov. 14, 1988	369	14.78	0.72		Ocean Flux Program Web site[c]
Sargasso Sea		4400	3200	31.8	64.2	Nov. 15, 1988	Nov. 11, 1989	361	13.25	0.61		Ocean Flux Program Web site[c]
Sargasso Sea		4400	3200	31.8	64.2	Nov. 11, 1989	Nov. 14, 1990	368	10.97	0.51		Ocean Flux Program Web site[c]
Sargasso Sea		4400	3200	31.8	64.2	Dec. 26, 1990	Dec. 20, 1991	359	14.72	0.69		Ocean Flux Program Web site[c]
Sargasso Sea		4400	3200	31.8	64.2	Dec. 20, 1991	Dec. 19, 1992	365	14.82	0.69		Ocean Flux Program Web site[c]
Sargasso Sea		4400	3200	31.8	64.2	Dec. 19, 1992	Dec. 16, 1993	362	11.52	0.60		Ocean Flux Program Web site[c]
Sargasso Sea		4400	3200	31.8	64.2	Dec. 16, 1993	Dec. 30, 1994	379	10.93	0.52		Ocean Flux Program Web site[c]
Sargasso Sea		4400	3200	31.8	64.2	Dec. 30, 1994	Dec. 19, 1995	354	12.81	0.59		Ocean Flux Program Web site[c]
Sargasso Sea		4400	3200	31.8	64.2	Dec. 31, 1996	Dec. 17, 1997	351	14.71			Ocean Flux Program Web site[c]
Canary Islands	CI	3600	1000	29.0	15.5	Nov. 25, 1991	Nov. 24, 1992	365	6.43	0.48		*Neuer et al.* [1997]
Canary Islands		3600	1000	29.0	15.5	Aug. 6, 1992	Aug. 6, 1993	364	10.83	0.86		*Neuer et al.* [1997]
Canary Islands		3600	3000	29.0	15.5	Nov. 25, 1991	Nov. 24, 1992	365	17.24	0.81		*Neuer et al.* [1997]
Canary Islands		3600	3000	29.0	15.5	Nov. 27, 1992	Nov. 27, 1993	365	18.76	0.87		*Neuer et al.* [1997]
Canary Islands		3600	3000	29.0	15.5	May 6, 1993	May 6, 1994	365	15.58	0.77		*Neuer et al.* [1997]
BOFS 2	BOFS-2	4860	3870	24.6	22.8	Oct. 14, 1990	Sept. 27, 1991	348	15.14	0.73		*Newton et al.* [1994]
EUMELI_M	EUM-M	3100	2500	21.0	31.0	Feb. 11, 1987	Jan. 6, 1988	329	74.75	7.68		*Bory and Newton* [2000]
EUMELI_M		3100	3000	21.0	31.0	Nov. 27, 1987	Nov. 23, 1988	362	58.63	1.91		*Bory and Newton* [2000]
EUMELI_O	EUM-O	4560	1000	18.0	21.0	Feb. 17, 1987	Feb. 15, 1988	363	11.48	0.61		*Bory and Newton* [2000]
EUMELI_O		4560	2500	18.0	21.0	Feb. 17, 1987	Feb. 15, 1988	363	11.52	0.50		*Bory and Newton* [2000]

Table 1. (continued)

Mooring Site	ID	Water Depth, m	Trap Depth, m	Latitude °N	Longitude °W	Date Start	Date End	Interval, days	Total Mass, g m^{-2} yr^{-1}	POC, g m^{-2} yr^{-1}	Trap Efficiency,[b] %	Source
Cap Blanc	CB	4094	730	21.1	20.7	Nov. 19, 1990	Nov. 19, 1991	365	31.02	3.76		*Fischer et al.* [2000]
Cap Blanc		4094	3557	21.1	20.7	Nov. 19, 1989	Nov. 19, 1990	365	59.19	1.88		*Wefer and Fischer* [1993]
Cap Blanc		4094	3557	21.1	20.7	Nov. 19, 1990	Nov. 19, 1991	365	32.09	2.36		*Fischer et al.* [2000]
Cap Blanc		3646	2195	20.8	19.8	March 22, 1988	March 22, 1989	365	67.17	2.74		*Wefer and Fischer* [1993]
Guinea Basin	GB	4522	859	1.8	11.1	April 4, 1990	April 7, 1991	368	30.60	2.94		*Fischer et al.* [2000]
Guinea Basin		4522	3965	1.8	11.1	April 4, 1990	March 30, 1991	360	44.20	2.18		*Fischer et al.* [2000]
Guinea Basin		4481	853	1.8	11.1	March 1, 1989	March 16, 1990	380	28.08	3.03		*Wefer and Fischer* [1993]
Guinea Basin		4481	3921	1.8	11.1	March 1, 1989	Feb. 25, 1990	361	37.29	2.19		*Wefer and Fischer* [1993]
Guinea Basin		3912	696	−2.2	9.9	March 16, 1990	March 16, 1990	380	9.41	1.09		*Wefer and Fischer* [1993]
Walvis Ridge	WR	2196	599	−20.0	−9.2	March 18, 1989	March 13, 1990	360	48.78	5.07		*Wefer and Fischer* [1993]
Walvis Ridge		2217	1690	−20.0	−9.2	March 4, 1988	March 16, 1989	377	59.06	6.08		*Wefer and Fischer* [1993]
Walvis Ridge		2196	1648	−20.0	−9.2	March 18, 1989	March 13, 1990	360	37.44	3.83		*Wefer and Fischer* [1993]
Walvis Ridge		2196	1648	−20.0	−9.2	March 25, 1990	April 9, 1991	380	23.66	2.77		*Fischer et al.* [2000]
Kerguelen Island	KI	1952	1588	−62.3	57.5	Dec. 1, 1983	Nov. 25, 1984	360	108.76	5.13		*Wefer et al.* [1990]
Kerguelen Island		1650	693	−62.3	57.5	June 14, 1984	June 14, 1985	365	25.90	0.71		*Wefer et al.* [1990]
Kerguelen Island		1992	687	−62.4	57.8	May 7, 1985	May 7, 1986	365	50.00	1.48		*Wefer et al.* [1990]
Weddel Sea	WS	5053	360	−64.9	2.6	Jan. 16, 1988	Jan. 15, 1989	365	35.24	3.49		*Wefer et al.* [1990]
Weddel Sea		5044	863	−64.9	2.6	Jan. 25, 1985	Jan. 25, 1986	365	0.26	0.03		*Wefer et al.* [1990]

[a] Flux stability index is calculated for dry weight, as defined in the text. OMEX, Ocean Margin Exchange; BOFS, British Ocean Flux Study; and EUMELI, Eutrophic, Mesotrophic and Oligotrophic Programe.
[b] Trap efficiencies calculated based on ^{230}Th and ^{231}Pa budgets from *Scholten et al.* [2001].
[c] Data were downloaded digitally from the Ocean Flux Program Web site (http://www.whoi.edu/science/MCG/ofp). For long-term analyses of these data, refer to *Deuser* [1986] and *Conte et al.* [2001].

depth; in this depth horizon, export production and sequestration diverge.

Quantification and characterization of the biological pump was a central goal of the JGOFS study, and a large amount of data is now available from long-term sediment traps deployed in the Atlantic Ocean. Though the use of sediment traps has its own caveats, its strength is that it collects sedimenting particles that reveal qualitative information that has greatly enhanced our understanding of biogeochemical cycling in the oceans. A major problem, as we emphasize, is the uncertainty of the efficiency of traps in collecting sinking particles [*Gust et al.*, 1994; *Scholten et al.*, 2001].

In this paper we use a compilation of sediment trap data from 27 sites in the Atlantic Ocean to determine the role of the biological pump in transfer of carbon to the ocean's interior and to investigate its regional characteristics and variability. We estimate the basin-wide potential of the biological pump for CO_2 sequestration from the atmosphere and its dependence on local production. We also concentrate on determining regional variations in flux characteristics and export efficiency, since these are important for predicting the response of the biological pump to changes in climatic forcing.

2. Materials and Methods

2.1. Database

Data have been collated from 27 sites (Figure 1; for site acronyms, see also Table 1) where particle interceptor traps were deployed in the Atlantic Ocean between 80°N and 65°S. Traps were conical, with an opening of ~0.5 m^2, deployed on bottom-anchored moorings for at least 1 year. Sample treatment varied in the addition of brine, use of fixative/poison, and methods of splitting and analytical procedure. Swimmers were removed from all samples either by manual picking under a binocular microscope or by passage through a sieve and subsequent rinsing. For details of mooring deployment and sample treatment the reader is referred to the publications listed in Table 1.

Individual samples were integrated over periods of between 7 and 65 days, with longer intervals during periods of low, constant flux. Dry weight, particulate organic carbon and nitrogen (POC and PON), carbonate, particulate biogenic silica, and lithogenic material were reported in mg m^{-2} d^{-1}. Inorganic carbon is calculated as 12% of calcium carbonate by weight, and opal is calculated from particulate biogenic silica using a molecular weight of 67.2 [*Mortlock and Fröhlich*, 1989]. For the Sargasso Sea (Ocean Flux Program (OFP) data) $CaCO_3$, POC/PON, and opal (for part of the data set) were determined on the <0.125 mm fraction (both the 0.37–0.125 mm and <0.37 mm fractions were analyzed separately and were used to calculate the <0.125 mm fraction). Opal fluxes are not corrected for leaching in the trap samples, as this was not measured in all studies. Where lithogenic fluxes were not reported, these are calculated as a difference between total flux and its biogenic components (lithogenic flux = mass flux − [carbonate + POC × 2.2 + opal]). The loss of POC to the dissolved phase can potentially cause a large underestimation of flux in shallow traps [*Noji et al.*, 1999; *Kähler and Bauerfeind*, 2001] but does not appear to be significant in deeper traps (P. Kähler, personal communication, 2000). Dissolved organic carbon (DOC) was not determined for most traps in this study.

Missing values were interpolated for intervals of up to 2 weeks using the mean value of the neighboring cups. Where gaps in the data occurred during low and constant flux (such as in winter), the mean value of that period from the entire data set was used if appropriate.

2.2. Annual Integrals

Since annual fluxes are used to quantify the relationship to surface productivity, care was taken to integrate over appropriate

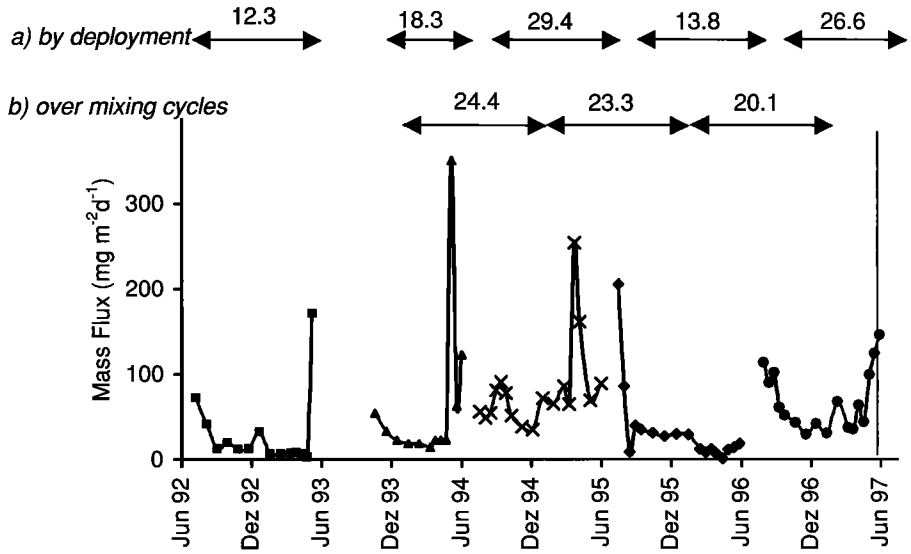

Figure 2. Long-term recordings of mass flux at 2000 m at station L2 (47°N, 20°W). Different symbols are data from consecutive deployments at the same site. Annual integrals are calculated by different means: (a) by deployment period or (b) over cycles of deep mixing (i.e., winter to winter).

time periods. Often, annual fluxes are reported as the mean flux over a deployment period extrapolated to 365 days, or else as a cumulative year of flux from trap deployment to trap recovery. Since deployment and recovery at sea are, for logistical reasons, frequently during high flux periods in summer, this method has the error of assigning a proportion of the peak flux to one year and another portion to the next. Here we integrate over deep mixing cycles (i.e., from winter to winter) since the nutrient budget, which determines annual new production, is set during deepest winter mixing. With some exceptions (see Table 1), integration was from February/March of one year (the time of deepest mixing in the North Atlantic) to the corresponding month of the following year. For sites in the Southern Hemisphere, integration was from May/June to May/June of the following year wherever possible (Kerguelen Island). For the OFP data from the Sargasso Sea, annual integrals were taken from November/December of one year to the next, which corresponds to periods of lowest, least variable flux [*Deuser*, 1996] and productivity [*Steinberg et al.*, 2001]. Particularly at sites where there is large seasonal variability in fluxes between years a comparison of these integration methods (over deployment periods versus over mixing cycles) yields large differences. For example (Figure 2), at site L2 (47°N, 20°W), annual fluxes over deep mixing cycles vary by 10% around the mean (mean 22.6 ± 2.2 grams dry weight (gdw) m^{-2} yr^{-1}), whereas they vary by 38% around the mean (mean 20.1 ± 7.6 gdw m^{-2} yr^{-1}) when integrated over deployment periods. Because of this potential bias we have calculated annual fluxes over deep mixing cycles even though this has reduced the amount of data used. The resulting integrals in Table 1 may thus differ from those reported in the source publications.

2.3. Primary/New Production Estimates

The selection of primary production estimates also proves to be no trivial matter. We compared estimates from the models of *Longhurst et al.* [1995], *Antoine et al.* [1996], and *Behrenfeld and Falkowski* [1997] for individual stations. Values were taken for a 1° × 1° grid centered on the trap sites that is representative of the mean surface variability in hydrographical conditions where particles settling to the traps are produced. For comparison with new production and f ratio we use data from *Oschlies and Garcon* [1998].

Although there is general agreement among models in the regional distribution of primary production, there is considerable site-specific discrepancy in the absolute values, particularly in polar regions where the estimates of *Longhurst et al.* [1995] are unaccountably high compared with regional estimates from nutrient budgets and models [*Rey*, 1991; *von Bodungen et al.*, 1995]. There is better agreement between *Antoine et al.* [1996] and *Behrenfeld and Falkowski* [1997], with the difference that the latter have higher estimates for the latitudinal bands between 30°–60°N and 30°–50°S, resulting in a higher basin-wide estimate of 13.3 Gt C yr^{-1} compared to 9.64 Gt C yr^{-1} of *Antoine et al.* [1996] for the area considered in this study. We use the data of *Antoine et al.* [1996] for better comparison with a number of recent publications [*Fischer et al.*, 2000; *Najjar and Keeling*, 2000; *Schlüter et al.*, 2000]. For additional comparison with the OFP flux data in the Sargasso Sea we extracted primary production data from the Bermuda Atlantic Time series Study (BATS) on-line database (http://www.bbsr.edu) and integrated values linearly for the annual cycles as given in Table 1.

2.4. Seasonality Index

We use an index for the seasonality/periodicity of flux as defined by *Berger and Wefer* [1990] and *Lampitt and Antia* [1997] and call it the flux stability index (FSI) as do *Lampitt and Antia* [1997]. The FSI is calculated by ranking the flux values according to their magnitude and by plotting the accumulated flux against time. The time in days for half of the total annual flux to arrive at the sediment trap is read off the graph and is the value of the FSI; low values thus indicate systems with highly pulsed export; high values indicate more constant sedimentation over time.

3. Results and Discussion

3.1. Efficiency of Sediment Traps

For the entire data set (n = 105), there is no clear relationship of POC flux with trap depth (Figure 3a). For open ocean situations,

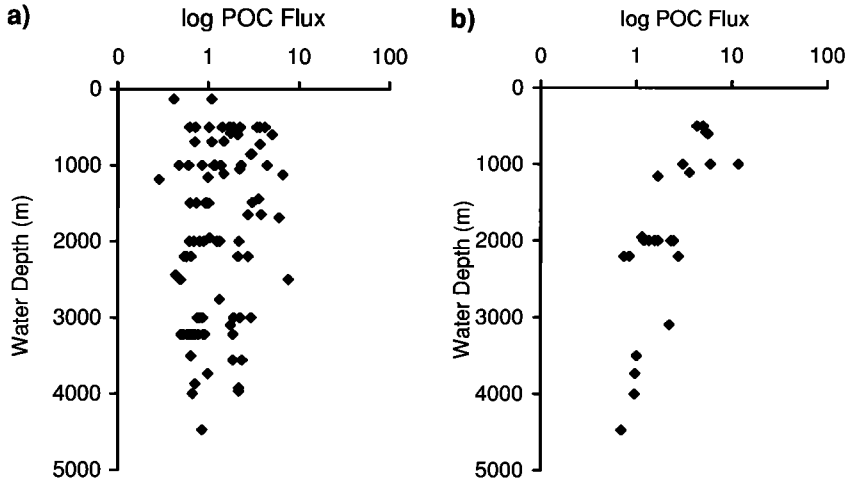

Figure 3. Relationship of particulate organic carbon (POC) flux to depth based on the entire data set in Table 1 (a) without correction for ^{230}Th flux and (b) using ^{230}Th corrected data only.

without strong lateral sources of particles, POC fluxes must decrease with depth since the degradation rate of POC (range of 3 days to 1 year [*Eppley et al.*, 1983; *Lande and Wood*, 1987]) is rapid compared to known particle sinking rates. Even trap bypassing by swimmers or the differing collection funnel at the surface [*Siegel and Deuser*, 1997; *Waniek et al.*, 2000] will, in the open ocean, affect the relative decrease of POC with depth but not cause its increase. For a number of stations, however, there is a decrease in flux above 1000 m, which may be a result of low collection efficiencies of the traps. Although fluxes measured in deep traps in the Sargasso Sea were seen to agree well with estimates from ^{230}Th and ^{231}Pa budgets [*Bacon et al.*, 1985], shallow traps are notoriously poor in performance [*Michaels et al.*, 1994; *Buesseler et al.*, 2000]. *Buesseler* [1991] found severe discrepancies (factor +10 to −10) between expected and measured ^{234}Th fluxes in drifting traps at 20–150 m depth over periods of 3–20 days. Since shallow drifting traps are exposed to a different hydrodynamic environment than those moored at several hundred meters depth, it is unclear as to how these results may translate to deep, moored traps.

For a subset of the data used here (n = 24), *Scholten et al.* [2001] show poor trapping efficiencies based on the expected annual fluxes of ^{230}Th. These range from under 50% (i.e., measured flux is 50% of expected flux) for traps shallower than 1000 m to between 64% and 123% for traps below 3000 m. Scaling the measured trap fluxes using these "correction" factors yields the expected decrease in POC and PON flux with depth (Figure 3b), though for a greatly reduced data set. Applying such a correction factor to all the measured variables assumes that particle trapping efficiency is based on hydrodynamic effects that bias all components of flux equally (but see also *Gust et al.* [1994] and *Buesseler et al.* [2000]). For the trap correction factors used here, we refer to a detailed discussion of their validity to *Scholten et al.* [2001], who find no clear relationships between ^{230}Th fluxes and those of specific variables, implying no discernible selectivity in trapping efficiency. We thus use the ^{230}Th correction for all measured components; because there is no consensus on this issue, we present results from stations with and without ^{230}Th corrections separately.

3.2. Interannual Variations in Flux

Since determination of empirical algorithms relating flux to production and water depth rely on annual means of productivity, we first examine to what extent interannual variations in flux can contribute to variations in export ratios. Interannual variability in fluxes is difficult to determine given the short time period of most studies (excluding the Sargasso Sea station). Table 2 summarizes the median values and variance of POC fluxes at single trap depths where at least 3 years of data are available. Annual fluxes vary little at the more tropical, oligotrophic sites L1, Canary Islands, and Sargasso Sea. The Walvis Ridge site is strongly influenced by the nearby lateral gradient in production from the adjacent coastal upwelling and the formation of "giant filaments" that can extend over the trap site in some years, causing large interannual variations [*Fischer et al.*, 2000]. At L3 the differences in annual fluxes between consecutive years is difficult to explain and may be caused by horizontal advection of particles from the nearby Rockall Plateau. Aside from WR and L3, annual variations are small compared to site-specific differences in flux.

In Figure 4 we examine interannual variations in the depth dependency of the export ratio, grouping sites L2 with 48°N and L1 with 34°N, since they were at the same location. There is encouraging similarity in fluxes at a single site and differences between sites. The Sargasso Sea site is unique in that there are long-term primary production data with approximately monthly resolution available from the BATS program [*Michaels and Knap*, 1996; *Steinberg et al.*, 2001] with which to compare annual variations in flux. The annual primary production at this site from the model estimate of *Antoine et al.* [1996] is 82.4 g C m^{-2} yr^{-1}, compared to estimates from the BATS data of 130, 157, and 186 g C m^{-2} yr^{-1} for the years 1989–1990, 1990–1991, and 1991–

Table 2. Median and Variance of Annual POC Fluxes From Sites Where 3 or More Years of Data Are Available

Site	Trap Depth, m	Median	Variance	n
L3	2200	1.81	1.49	3
L2	2000	2.31	0.48	3
Canary Island	3000	0.81	0.003	3
L1	2000	1.35	0.03	3
Sargasso Sea	500	1.65	0.29	4
Walvis Ridge	1500	0.94	0.02	6
	3000	0.67	0.02	14
	1690	3.83	2.86	3

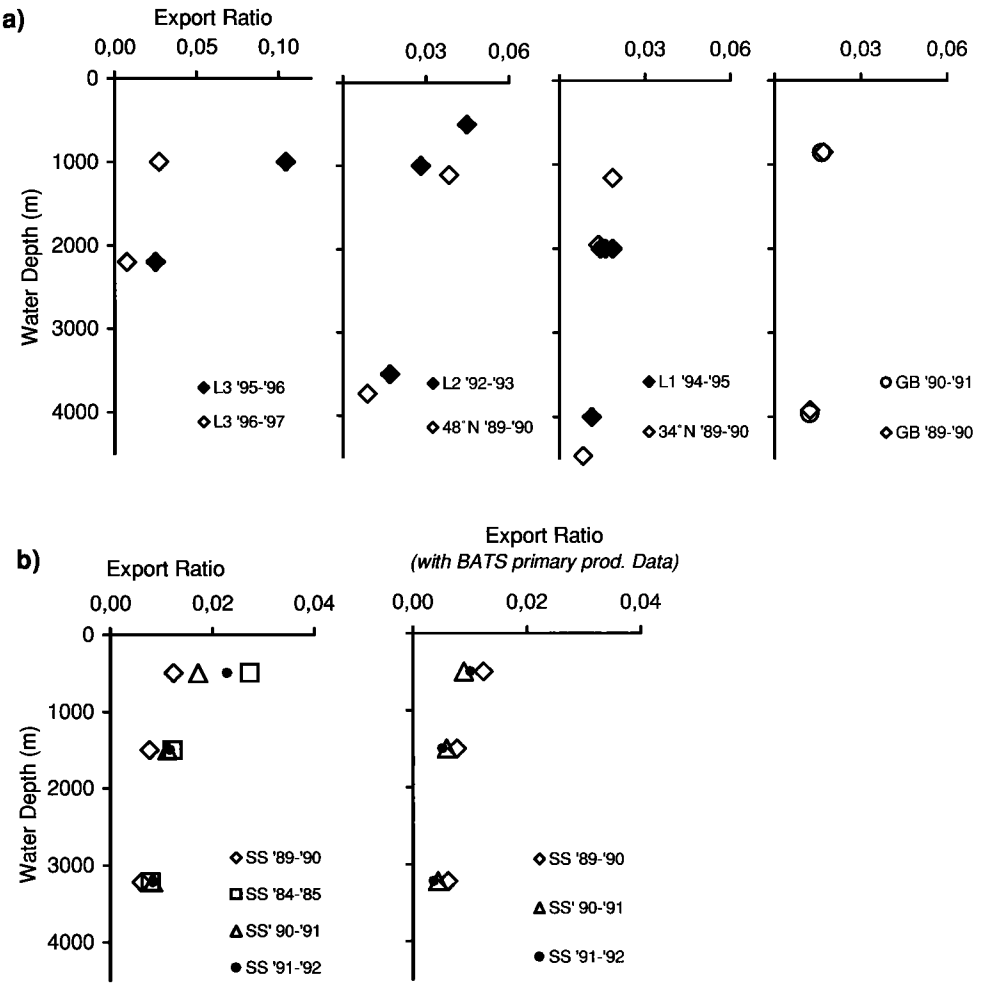

Figure 4. (a) Changes in the export ratio (POC flux/primary production) with depth at sites where data are available for >1 year. (b) Data plots for the Sargasso Sea (left) using model estimates of primary production from *Antoine et al.* [1996] and (right) using primary production estimates from the BATS site.

1992, respectively (integrated over the time periods listed in Table 1). Variations in flux between these years reflect these changes in annual production, such that differences in export ratio between years based on a single model estimate (Figure 4b, left) are largely lost when using site-specific real-time data (Figure 4b, right). There are precious few sites for which such data are available, and these results point to an extremely tight coupling of production with flux over annual timescales.

In summary, we conclude that although there are some interannual variations in flux and the extent to which it decreases with depth, these are smaller than the differences between sites, allowing intersite comparisons based on the available data.

3.3. Relationship of Export Ratio to Depth and Primary Production

By applying correction factors to account for low trapping efficiencies and in view of the generally low interannual variations in flux we proceed to examine regional and basin-wide relationships based on a reduced, but more robust, data set. For depth-dependant degradation of fluxes we apply the model

$$J_{\mathrm{Corg}} = c\mathrm{PP}^a Z^b \tag{1a}$$

as used by *Betzer et al.* [1984] to derive an algorithm relating flux to productivity and depth, where J_{Corg} is the organic carbon flux (g C m^{-2} yr^{-1}) at depth z (m), PP is primary production (g C m^{-2} yr^{-1}) and a, b, and c are constants. Data used for the fit are those with ^{230}Th correction only ($n = 24$). This reduced database is distributed between 33°N and 54°N, representing a range of production from the oligotrophic gyre to the subpolar North Atlantic.

Using model II least squares regression, the best fit yields

$$J_{\mathrm{Corg}} = 0.1\mathrm{PP}^{1.77} z^{-0.68} \tag{1b}$$

$$R^2 = 0.53, n = 24.$$

The exponent of the depth term z (−0.68), which represents the decrease in POC flux with depth, is similar to the empirically determined values of *Betzer et al.* [1984] and *Pace et al.* [1987] from the oligotrophic Pacific (−0.628 and −0.734, respectively). Figure 5a compares the depth dependence of export ratio (ER) for these and other empirical algorithms [*Suess*, 1980; *Betzer et al.*, 1984; *Pace et al.*, 1987; *Berger et al.*, 1987] calculated for a primary production value of 100 g C m^{-2} yr^{-1}. With the exception of the *Suess* [1980] algorithm, there is little difference among the compared algorithms, reflecting the general consistency in POC

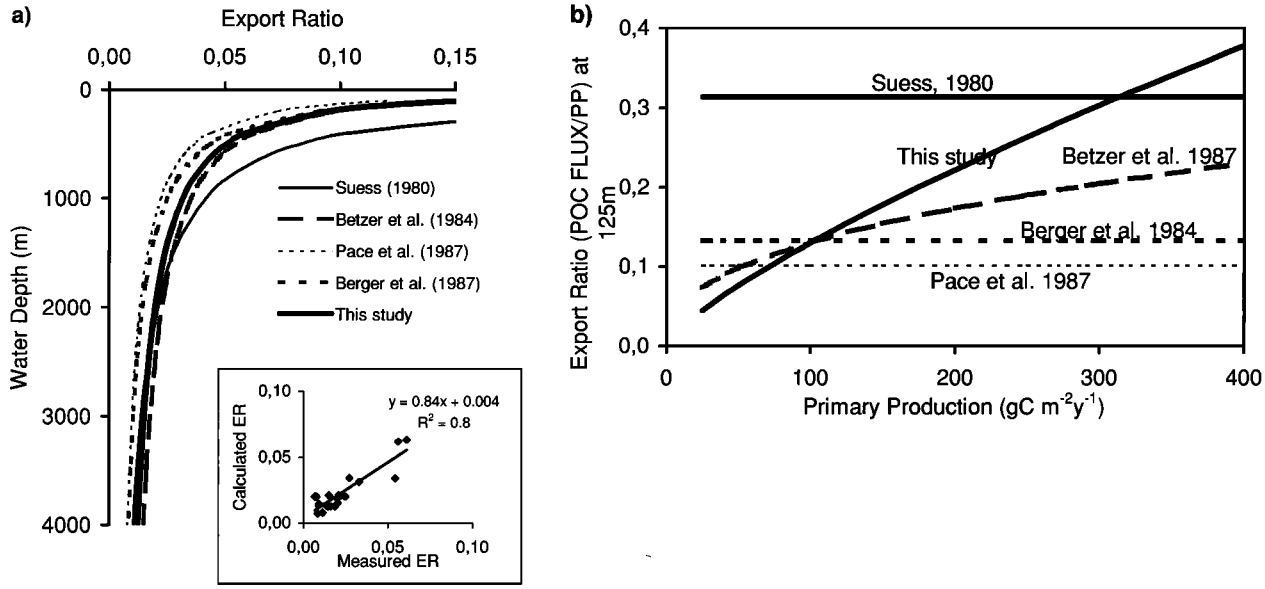

Figure 5. (a) Relationship between export ratio and water depth using algorithms from the literature and from this study using ^{230}Th corrected data only. Insert shows regression of measured flux at trap depth and calculated flux using the algorithm presented in this study. (b) Changes in the export ratio calculated at a depth of 125 m using the algorithms presented in Figure 5a. $ER_{125} = cPP^{a-1} \times 125^{b}$. Thus, when $a = 1$, ER_{125} is constant.

degradation with depth. Major differences are seen, however, when comparing the export ratio at the base of the euphotic zone (taken as 125 m), which ranges between 0.12 [*Pace et al.*, 1987] and 0.39 [*Suess*, 1980] over the range in primary production between 50 and 400 g C m^{-2} yr^{-1}, depending on the algorithm used. The choice of algorithm and data on which it is based will thus have a significant impact on calculation of basin-wide export.

It is instructive to recall that the algorithms shown in Figure 5 are based on data from different sites and integrated over different periods. Although reported in units of flux per unit area and year [*Suess*, 1980; *Betzer et al.*, 1984; *Berger et al.*, 1987], these studies use short-term (days to weeks) measurements of flux and relate them to contemporaneous productivity integrated over the euphotic zone. Yet it is known that production and flux are not in balance on short timescales [*Lohrenz et al.*, 1992] due to nutrient and particle retention by a seasonally variable food web [*Wassmann*, 1998; *Boyd and Newton*, 1999].

Use of any single algorithm, aside from yielding quantitative differences in export, implies that there is a globally applicable export ratio to a particular depth. However, it has been demonstrated that regional differences in export ratio exist and are related to the seasonality of export, with more pulsed export systems (typical for temperate and polar regions) exporting about twice as much of their production as systems with more constant export (typical for oligotrophic tropical systems) [*Berger and Wefer*, 1990; *Lampitt and Antia*, 1997] The low export ratio of *Pace et al.* [1987], for example, may thus reflect the oligotrophic conditions at the Vertical Transport and Exchange Study (VERTEX) site and thus may not be globally applicable.

Over steady state cycles, export at the base of the euphotic zone approximates new production (the fraction of primary production based on allochthonous nutrient sources [*Eppley and Peterson*, 1979]). Over the range of primary production in the open ocean (50–400 g C m^{-2} yr^{-1}), annually averaged f ratios (the ratio of new to total production) range from <0.1 to ~0.5 and can be compared to the export ratio at 125 m (ER_{125}), the nominal depth of the euphotic zone. Variable f ratios are an inherent feature of pelagic systems resulting from regional differences in physical forcing, degree and duration of stratification, and degree of recycling by the pelagic food web. Assuming that export is linearly related to production (i.e., $PP^{1.0}$) implies that ER_{125} will remain constant for all values of PP, as is the case for the algorithms of *Pace et al.* [1987], *Berger et al.* [1987], and *Suess* [1980] (Figure 5b). The higher dependency on PP given by *Betzer et al.* [1987] ($PP^{1.41}$) and this study ($PP^{1.77}$) yields corresponding changes in ER_{125} (and, by implication, f ratios) from <0.1 to 0.23 and from <0.1 to 0.38, respectively, over a range of PP from 50 to 400 g C m^{-2} yr^{-1}. This is consistent with the early estimates of *Dugdale and Goering* [1967] and *Eppley and Peterson* [1979] and also with mean annual f ratios estimated for oligotrophic and mesotrophic environments [*Campbell and Aarup*, 1992; *Dugdale et al.*, 1992] by independent means. This is also in agreement with the increase in export ratio (normalized to 1000 or 2000 m depth) with increasing primary production, as shown by *Lampitt and Antia* [1997] and *Fischer et al.* [2000].

3.4. Regional Differences in Export Ratio (ER) With Depth

A main aim of this study was to examine regional differences in the efficiency of the biological pump. Previous studies have analyzed such differences [*Lampitt and Antia*, 1997; *Fischer et al.*, 2000] but have been unable to identify variations in the export function with depth, since data were normalized to a single depth.

A total of 10 stations in our data compilation have annual fluxes from two or more depths that allow a regional comparison. In Figures 6a, changes in ER with depth for five stations at three sites on a meridional transect at 20°W (33°N to 54°N) are presented, where data have been corrected by *Scholten et al.* [2001] using the ^{230}Th method. In Figure 6b and 6c a further five stations are compared where such a correction is not available.

For the ^{230}Th corrected data, there is a clear latitudinal trend in variations of export ratio with depth. It is worth noting that the geographic locations of stations L1 and L2 [*Kuss and Kremling*, 1999] are identical to those of stations 34°N and 48°N [*Honjo and Manganini*, 1993] but were occupied during different years, using different moorings and methodology, yet the data cluster to show

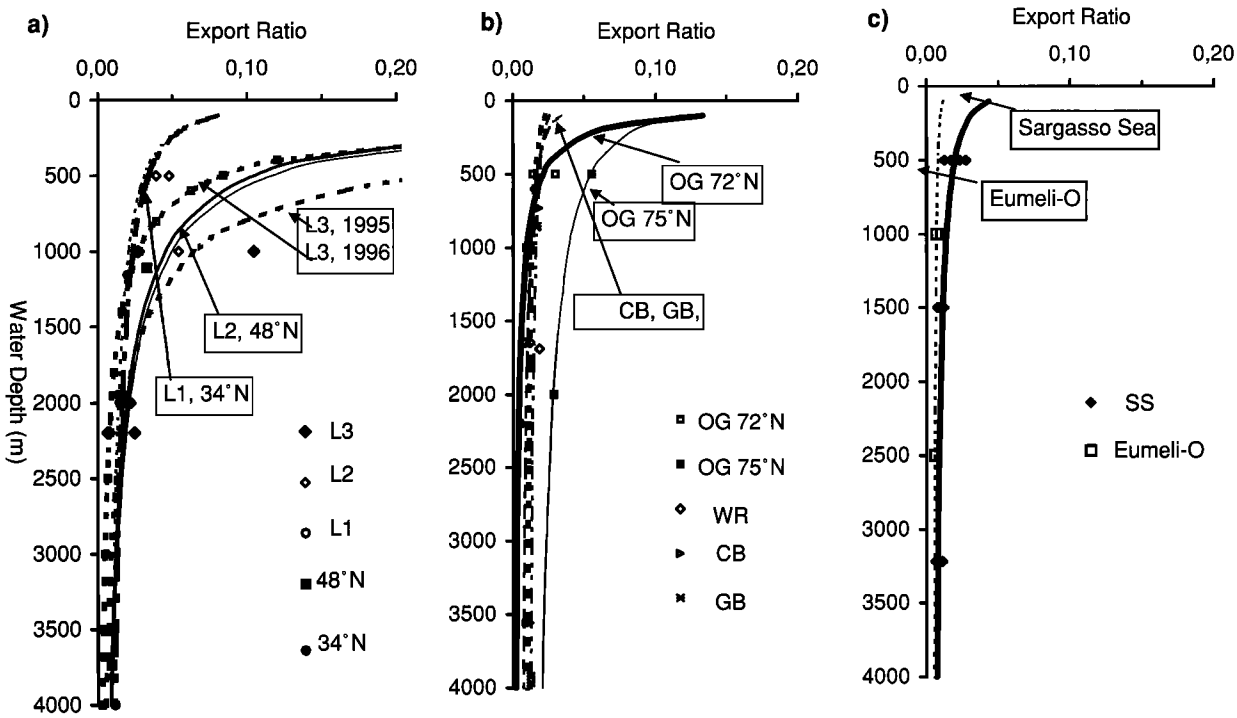

Figure 6. Changes in export ratio with water depth at individual sites. Lines are regressions through the data as per equations (1a) and (1b). Data from 500 m at L2 have not been used for the regression.

clear regional variations. The oligotrophic site at 33–34°N has a factor of 2 lower export ratio at 1000 m depth than the North Atlantic Bloom Experiment (NABE) site at 47–48°N. At 54°N (L3), there appears to be considerable interannual variability between the two successive years (1995 and 1996). This causes differences in the range of ER at L3, but both years show similar strong depth-dependent flux losses. As we show in section 3.6, these differences between sites are also reflected in the composition of sedimenting particles and the seasonality index, giving us some confidence in interpretation of site-specific differences.

Figures 6b and 6c show data from sites where ^{230}Th correction is not available. On the basis of the ER and depth-dependent degradation rates these can be roughly grouped in three clusters; two sites in the East Greenland Sea (OG and OG 75°N), four sites in the subtropical Atlantic (Guinea Basin, Cap Blanc, Walvis Ridge, and the Sargasso Sea), and one site in the oligotrophic North Atlantic gyre (EUMELI-O). The OG 75°N site experiences seasonal ice coverage where the growth period is limited to a few months a year; here we see highest export ratios. This is probably due to the most rapid transfer of particles to depth that is characteristic for ice margin conditions where grazing is low and particle export can be rapid. The open ocean site OG at 72°N also has high export ratio above 500 m, with a sharp decrease to 2000 m. The second group of sites in the subtropical Atlantic shows low export ratios and little flux degradation with depth; export ratios are uniformly below 0.02 (as reported by *Fischer et al.* [2000]). The most oligotrophic site in the subtropical North Atlantic gyre (EUMELI-O) shows the lowest export ratios encountered (0.07 and 0.056 at 1000 and 2500 m, respectively).

3.5. Comparison of Export Production to New Production

A major concern in extrapolating fluxes measured well below the euphotic zone (≥500 m) to a depth of 125 m is that most of the organic carbon degradation occurs between these depth horizons. Essentially, all algorithms including ours have the weakness that they use relatively small variations in flux at greater depths to extrapolate to larger variations near the surface. We thus find it instructive to compare the algorithm presented here to modeled new production estimates that do not share this caveat.

Extrapolating measured differences in the export function with depth upward to the base of the euphotic zone shows clear regional differences in export (new) production. We have fitted the flux function (equations (1a) and (1b)) to the regional data to extrapolate to export ratio at 125 m (ER_{125}, the euphotic depth used by *Oschlies and Garcon* [1998] to calculate new production)]. The resulting curves are statistically weak, based as they are on so few data points, and the curvature is largely determined by the relatively small variation in ER ≥ 500 m. Nonetheless, we compare the ER_{125} to the *f* ratio at the same depth using model estimates of new production [*Oschlies and Garcon*, 1998] and total production [*Antoine et al.*, 1996]. With the exception of data from the Sargasso Sea, there is good agreement between the estimates (Figure 7a). The Sargasso Sea site lies near the strong gradient in new production at the northwestern edge of the subtropical gyre, with higher new production than in the gyre itself. New production estimates for this site of 0.33 mol N m^{-2} yr^{-1} [*Altabet*, 1989], 0.56 mol N m^{-2} yr^{-1} [*Jenkins*, 1988], and 0.50 mol N m^{-2} yr^{-1} [*Oschlies and Garcon*, 1998] are an order of magnitude higher than the 0.04 mol N m^{-2} yr^{-1} extrapolated from the trap data. At the nearby BATS site, *Lohrenz et al.* [1992] estimate new production at 0.1–0.11 mol N m^{-2} yr^{-1} from export to shallow (125 m) drifting sediment traps (but note large collection biases at these depths from *Buesseler* [1991]).

High new production/export systems are characteristic of high latitudes, where bloom-forming plankton such as diatoms often dominate the pelagic community. Such bloom-and-bust scenarios have pulsed export and a strong seasonality in flux; this is seen in the strong correlation between the flux seasonality index (FSI), the

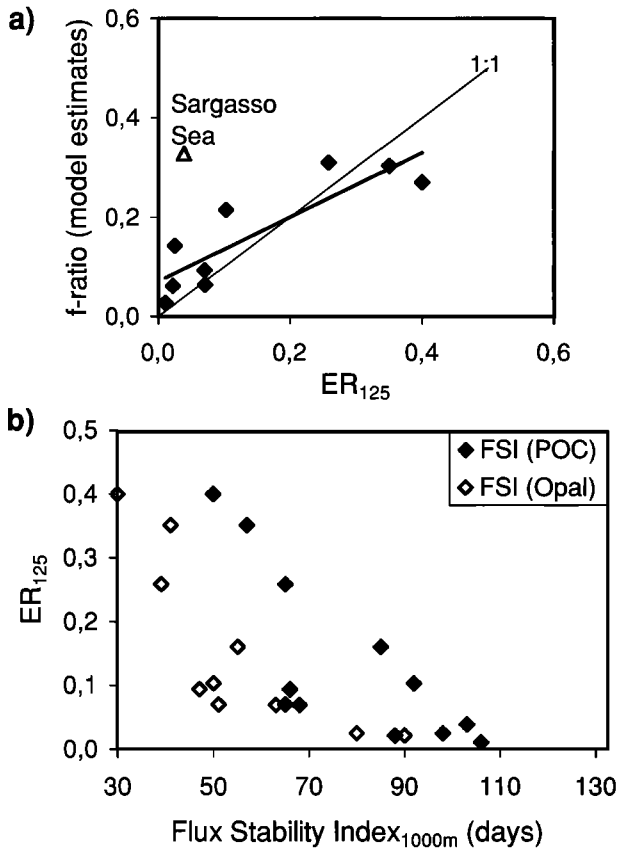

Figure 7. (a) Comparison of export ratio at 125 m (ER_{125}) using only ^{230}Th corrected data with f ratio using new production estimates of *Oschlies and Garcon* [1998] and primary production of *Antoine et al.* [1996]. Least squares regression yields $y = 0.65x + 0.07$, $r^2 = 0.76$, $n = 9$. The Sargasso Sea was not included in the regression. (b) Relationship of ER_{125} to flux stability index based on POC and opal fluxes. FSI has been normalized to 1000 m using regressions based on the entire data set. Low FSI values indicate pulsed export, with high values indicating more constant export with time.

export ratio (ER_{125}), and the rate of degradation of POC with depth (the z exponent of equations (1a) and (1b)) (Figure 6). Contrary to what is seen on the short timescales of such pulses, where a pulse of material can rapidly reach the seabed [*Lampitt*, 1985], on an annual timescale, high export systems do not provide proportionally more material to the deep sea.

Despite large differences in shallow fluxes (by a factor of 24, from 0.5 to 11.65 g C m^{-2} yr^{-1}), below 3000 m, there is much less variation between sites (by a factor of 4.4, from 0.5 to 2.4 g C m^{-2} yr^{-1}). This implies the presence of an active and efficient midwater community, capable of and adapted to feeding on sinking particles until some minimal, threshold value of particles is reached that ultimately settle to the abyssal seabed. This underscores the importance of this "twilight zone" (the depth horizon between the bottom of the euphotic zone and ~2000 m) that dampens the quantitative relationship between surface productivity and deposition to the seafloor. The fourfold regional difference in deep-ocean fluxes reported here is of the same range as deep-sea benthic flux patterns [*Jahnke*, 1996]. In both their quantitative and marker signals, benthic fluxes and their accumulation in the sediments harbor valuable proxies that are used to reconstruct paleoproductivity scenarios [*Sarnthein et al.*, 1992; *Wefer et al.*, 1999].

3.6. Regional Characteristics of Export and Composition of Sinking Particles

Regional characteristics based on the above analyses are still potentially influenced by methodological biases. We therefore make another comparison on the basis of the composition of sedimenting particles, by conducting principal component analyses (PCA) on the dry weight (DW)-normalized POC, PON, opal, and carbonate fluxes (i.e., fluxes expressed as a fraction of DW flux) for the entire data set. The PCA is a technique of linear statistical predictors that has been widely applied in environmental sciences [*Jackson*, 1991]. All statistical calculations were made using log-transformed data to improve the homogeneity of variance. The first two principal components span a two-dimensional plane onto which each point can be projected. The plane is chosen in such a way that the variance of these projections is as large as possible. The position of each projected point on this plane can be visualized in the form of a so-called biplot (Figure 8). The biplot shows the correlation between each mooring and the first two principal components by means of a vector. The length of each vector is equivalent to the fraction of the total variance that is explained the first two principal components; thus all the variance in the concentration is explained by the first two principal components when a vector reaches the drawn unit circle.

On the basis of the temporal mode and depth dependency of flux (Figure 8a), sites geographically close to each other are similar and cluster separately from other groups of sites. Grouping of L1 with 34°N and L2 with 48°N is evident as is the commonality between equatorial sites Cap Blanc and Guinea Basin and sites in the oligotrophic equatorial North Atlantic Gyre (Sargasso Sea and Eumeli_O). The polar OG 75°N site, under seasonal ice cover, and OG in the open Greenland Sea at 72°N are dissimilar with respect to export characteristics, primarily due to the low z exponent at OG 75°N. This provides a first step toward the approach of defining geographical provinces according to their characteristics of the biological pump, however, the spatial coverage of data is too weak to allow delineation in the form of biogeochemical provinces as described by *Longhurst* [1998].

On the basis of flux composition (Figure 8b), there is a clear clustering of sites with polar regions distinguished from nonpolar by their high opal (mean 27% DW, range 5.2–45%) and low carbonate (mean 11.7% DW, range 4.8–21%) content. Outside of polar regions, opal accounts for <10% (with the exception of the Sargasso Sea at 13.7%) and carbonate for over 50% of sedimenting matter. As expected, highest opal content (45% DW) is seen in the Southern Ocean (KG), whereas in the Arctic Atlantic (FS, PI, OG75°N) this ranges from 5.7 to 14% DW.

Along a transect at 20°W in the eastern North Atlantic, stations L3, L2, and L1 show a progressive decrease in opal: carbonate ratios going from north to south [*Kuss and Kremling*, 1999]. The lack of cohesion in traps at different depths from L3 and L2 reflects differences in POC content from above 10% above 1000 m to below 5% at depths >2000 m. Interestingly, there is a difference in composition of flux between the mooring sites 48°N and L2 and 34°N and L1 that otherwise show strong similarity in flux characteristics (Figure 8a). We compare the opal:carbonate ratio in sedimenting material below 1000 m for the time period between 1989, when the moorings 34°N and 48°N were deployed, and 1994–1997, when moorings L2 and L1 were deployed at the same sites. There is a clear decrease in opal:carbonate ratios during this 8-year period, which is similar to the decrease in this ratio shown by *Deuser et al.* [1995] in the Sargasso Sea between 1978 and 1991 (Figure 9). *Deuser et al.* [1995] attempt to relate this to long-term changes in wind speed, implying that it may be a response to regional climatic variations. If the phenomenon is common to a larger area of the North Atlantic, this may implicate some common cause related to large-

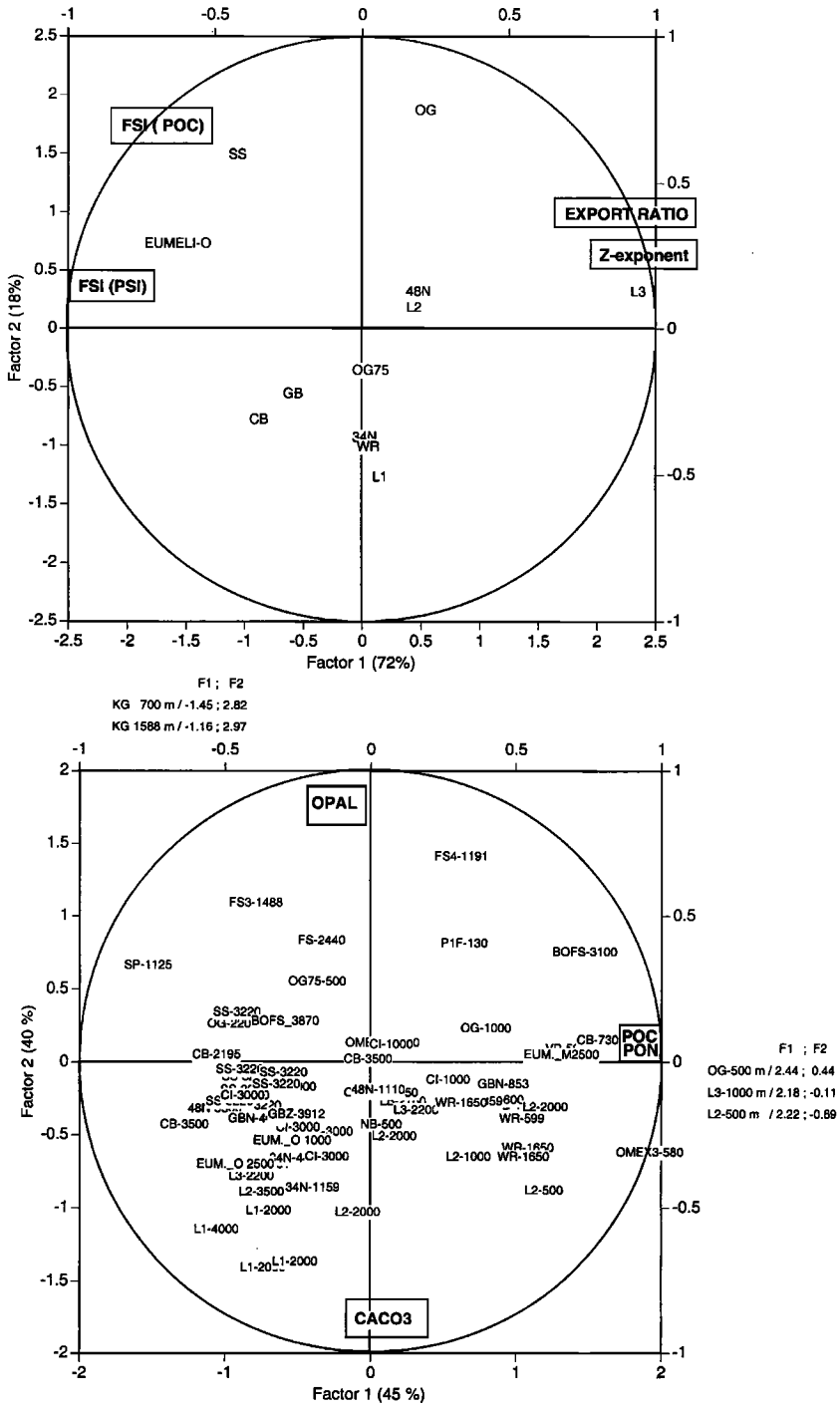

Figure 8. Principal component analysis based on (a) the characteristics of flux (export ratio, flux stability index, and value of the depth exponent of z in equations (1a) and (1b) (see text) and (b) based on the DW-normalized fluxes of POC, PON, carbonate, and opal in sedimenting particles.

scale physical forcing, perhaps tied to the North Atlantic Oscillation. It is worth noting that as reported by *Deuser et al.* [1995], the alteration in opal:carbonate ratios is primarily due to a drop in opal fluxes (by ~50%) rather than an increase in carbonate flux (by ~17%).

At 2000 m depth, similar POC fluxes are registered, but POC:PIC ratios drop by 7 and 17% between 1989 and 1996 at 48°N and 34°N, respectively. The decrease in opal fluxes is thus accompanied by decreased POC flux and lower efficiency of sequestration through alteration of the rain ratio of sedimenting particles. True time series measurements in the ocean are rare. Yet if the pattern seen in this study reflects a general change in structure of the pelagic community resulting from changes in physical forcing at the surface, the implications are that changing surface mixing will change not just the absolute level of new production and thus export but also the efficiency with which the

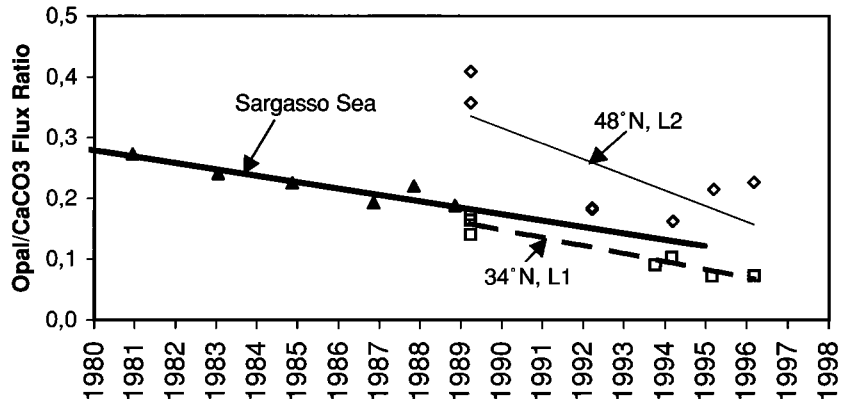

Figure 9. Long-term trend in the opal:carbonate ratio in sedimenting particles from the Sargasso Sea, at 47°N, 20°W, and from 34°N, 21°W. The line for the Sargasso Sea represents that derived by *Deuser et al.* [1995] with a slope of 0.0105 yr^{-1}. The slope of the lines for 48°N/L2 and 34°N/L1 are 0.026 yr^{-1} and 0.015 yr^{-1}, respectively.

biological pump exports to depth, providing a feedback mechanism to climate change.

3.7. Rain Ratio

Since one of the aims of this study is to derive an estimate of basin-wide export flux as it is related to drawdown of atmospheric CO_2 by the biological (tissue and carbonate) pump, we examine regional and depth-related changes in the ratio of organic to inorganic carbon exported (POC:PIC, rain ratio, RR). Photosynthesis decreases the pCO_2 of surface waters, whereas calcite production increases pCO_2, altering the carbonate equilibrium of seawater such that at a molar POC:PIC ratio of 0.6:1, there is no net change in pCO_2 [*Kano*, 1990]. Within the upper ocean this ratio differs both horizontally (regionally) and vertically, with photosynthesis exclusively within the euphotic zone and carbonate also produced by deeper-living zooplankton. Additionally, there is substantial and differential degradation of both POC and calcite within the upper 1000 m of the water column (see Figure 5) [*Milliman et al.*, 1999] that changes the ratio of POC:PIC in sinking particles.

Highest rain ratios are seen at polar sites and at continental margins (Figure 10a). Outside these regions, for the nonpolar, open ocean data, there is a good correlation of rain ratio with depth:

$$\mathrm{POC:PIC} = 7.39 - 0.83\ln(Z), r^2 = 0.67, n = 84, \quad (2)$$

where POC:PIC is the rain ratio at water depth z (in m). This gives a mean rain ratio of 3.7 at 125 m. Significantly higher rain ratios from the polar oceans and continental margins underscore their importance in the global carbon cycle since they are able to more efficiently sequester CO_2 for each unit of organic carbon produced.

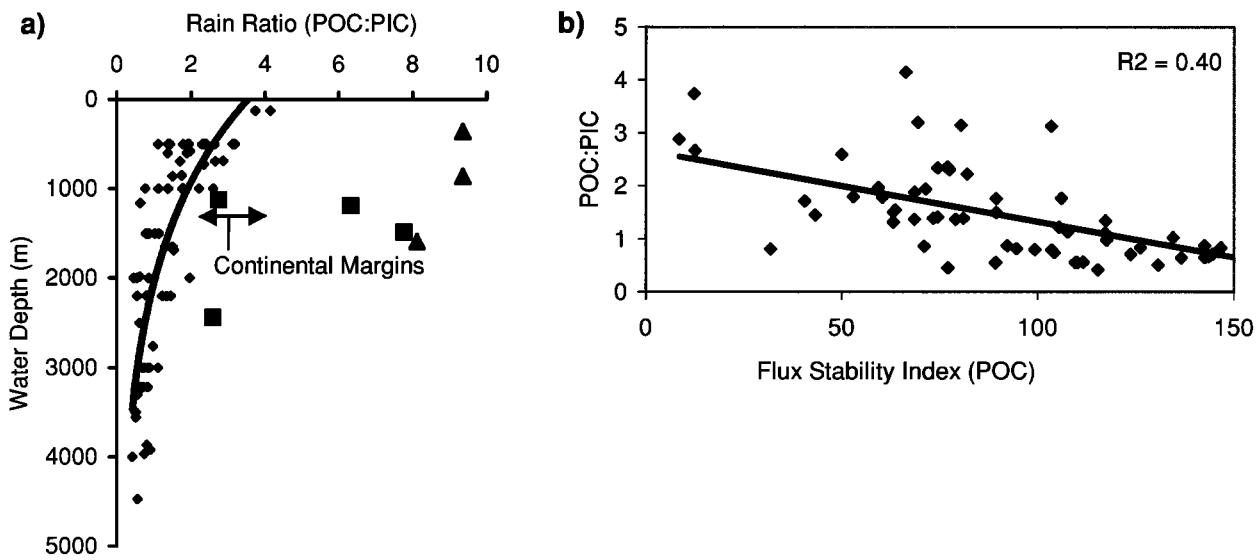

Figure 10. (a) Changes in rain ratio (POC:PIC in sedimenting particles) with depth. The least squares regression (see text) is based on nonpolar data only (diamonds). The polar Arctic (squares) and polar Antarctic (triangles) regions are shown separately. The box indicates the range of rain ratio in midwater depths at Atlantic continental margins as summarized by *Antia et al.* [1999]. (b) Relationship of rain ratio to flux stability index based on POC fluxes.

Within the nonpolar open ocean, and within the scatter of the data used to determine equation (2), there is a weak latitudinal trend of higher rain ratio at higher latitudes. These high-latitude areas, which have higher export ratios and more pulsed export (Figure 10b) are more efficient net carbon exporting systems than the low-latitude systems. The ultimate gradient in pCO_2 between the surface ocean and atmosphere that can be equilibrated through gas exchange must take the rain ratio into account at the depth of maximal winter mixing. We estimate the net effect on surface seawater pCO_2 by using the opposing processes of organic and inorganic carbon export at the mixed layer depth that we term the "effective carbon flux," defined as the carbon export at the winter mixed layer depth that drives a potential drawdown of CO_2 from the atmosphere to the ocean:

$$J_{\text{eff}} = J_{\text{POC(WML)}}\left[\left(\text{RR}_{\text{(WML)}} - 0.6\right)/\text{RR}_{\text{(WML)}}\right], \qquad (3)$$

where J_{eff} is the effective carbon flux, $J_{\text{POC(WML)}}$ is the POC flux calculated according to equation (1b) to the WML depth, $\text{RR}_{\text{(WML)}}$ is the rain ratio at the WML depth, calculated according to equation (2), and 0.6 is the RR at which $\Delta pCO_2 = 0$.

An obvious effect of the variations in rain ratio with depth is that the difference between J_{Corg} and J_{eff} widens with increasing water depth. Calculated immediately below the euphotic zone, at a nominal depth of 100 m, J_{eff} amounts to 84% of J_{Corg}. At 600 m depth the effective carbon flux is reduced to 71% of J_{Corg}, reflecting the increase in the carbonate fraction of export with depth. As a consequence, the sequestration flux is highest at low latitudes where maximal annual mixing is shallow, even though the "efficiency" of export, through higher rain ratios, is larger at polar latitudes. Changes in the depth of maximal ventilation will thus have multiple effects on the biological export of carbon: shoaling of the maximum mixed layer depth will cause a strong (exponential) increase in export ratio (Figure 5) as well as a smaller increase in net sequestration due to higher rain ratios. These will be counteracted by decreased nutrient inputs and decreased net production.

3.8. Basin-wide Flux Calculation

Next we calculate the carbon fluxes for the Atlantic Ocean between 65°N and 65°S and 100°W and 20°E, with a resolution of 1° × 1°, excluding marginal seas (Baltic and Mediterranean Seas and Hudson Bay). The total area of integration is 8.32×10^{13} m^2; note, however, that the areas applied in estimating individual fluxes differ slightly depending on the availability of input data (see Table 3). A further assumption was made to account for the continental margins where the WML depth impinges on the slope. These areas are characterized by high productivity due to topographically induced upwelling; however, the majority of export production remineralized on the shelf and upper slope does not contribute to long-term sequestration of carbon [*Antia et al.*, 1999]. Thus we take the slope depth to the depth of maximum winter mixing as the continental boundaries of our calculations.

Input data consist of annual primary production [*Antoine et al.*, 1996] and maximum mixed layer depths from monthly resolved data based on climatological temperature and salinity data [*Monterey and Levitus*, 1997]. The mixed layer depth is defined as the change in density with respect to the surface by 0.125 kg m^{-3}.

Results of basin-wide flux estimates are given in Table 3. J_{125} is the particle export flux calculated using equation (1b) at a depth of 125 m. J_{WML} is the corresponding flux at Z_{WML}, the maximum depth of the mixed layer. In the tropics, Z_{WML} becomes shallower than 125 m; hence the property J_{exp} is estimated as the maximal value of J_{125} and J_{WML} (J_{exp} = max (J_{125}, J_{WML})). The remineralization between the productive layer (min (Z_{WML}, Z_{125})) and Z_{WML}, $R_{\text{EXP - WML}}$, is estimated from areal integrations of J_{exp} and J_{WML} to avoid errors due to slightly different areas on which these were based:

$$R_{\text{EXP-WML}} = \left(\Sigma J_{\text{exp}}/A_{\text{exp}} - \Sigma J_{\text{WML}}/A_{\text{WML}}\right)A_{\text{WML}},$$

where A_{exp} and A_{WML} are the areas for which J_{exp} and J_{WML} were calculated. J_{eff}, the effective carbon flux, is calculated according to equation (3).

Table 3. Carbon Fluxes in the Atlantic Ocean[a]

	Flux, Gt C yr^{-1}	Area, × 10^{13} m^2
PP	9.64[b]	
J_{125}	1.68	8.32
J_{WML}	2.94	8.28
J_{exp}	3.14	8.32
$R_{\text{EXP-WML}}$	0.18	(8.32)
J_{eff}	2.47	8.26

[a] PP, primary production from *Antoine et al.* [1996]; J_{125}, POC flux calculated to a depth of 125 m as per equation (1b); J_{WML}, POC flux at the maximum depth of the winter mixed layer; J_{exp}, maximal value of J_{125} and J_{WML} when the mixed layer depth is shallower than 125 m; $R_{\text{EXP - WML}}$, remineralization between the productive surface layer and the winter mixed layer depth; J_{eff}, effective carbon flux as defined in text and calculated according to equation (3)

[b] *Antoine et al.* [1996] estimate the integrated primary production of the Atlantic to be 9.86 Gt C yr^{-1} (27% of their global primary production of 36.5 Gt C yr^{-1}). Their estimate is based on a slightly different regional definition of the Atlantic Ocean as compared to the one used in our study.

Plate 1 shows the resulting basin-wide flux calculations from 65°N to 65°S. Over this area, primary production is 9.64 Gt C yr^{-1}, and J_{exp} amounts to 3.14 Gt C yr^{-1} or a mean export (f) ratio of 0.33 (Table 3). This value lies between the mean global f ratio from applying the *Eppley and Peterson* [1979] curve to estimates of primary production (mean f ratio 0.3 [*Falkowski et al.*, 1998]) and that from the eddy-permitting North Atlantic model of *Oschlies and Garcon* [1998] (f ratio 0.43 between 8°S and 65°N). Export production of 3.14 Gt C yr^{-1} for the area considered is, however, proportionally overly large compared to the spring-summer global new production estimates based on net air-sea O_2 flux (4.5–5.6 Gt C yr^{-1} [*Najjar and Keeling*, 2000]). The basin-wide effective carbon flux J_{eff} amounts to 2.47 Gt C yr^{-1}.

The regional distribution of J_{exp} (Plate 1a) depicts high latitudes having a mean export (new) production ~10 times higher than the oligotrophic gyres. This pattern changes in terms of the effective carbon flux J_{eff} (Plate 1b), where the effects of in-depth regional variations of winter mixing and changes in the rain ratio with depth are incorporated. Because of the high rain ratio at shallow winter mixed layers (i.e., when WML is 125 m), such as in the tropics, $J_{\text{exp}} \approx J_{\text{eff}}$ in these regions. In a global budget the sequestration flux due to particulate export must be balanced against the outgassing of CO_2 from subthermocline, upwelled water. The net effect of changes in upwelling intensity on the air-sea exchange of CO_2 through simultaneous changes in nutrient input, maximal ventilation, and J_{eff} is largely unclear. In the subtropical and temperate Atlantic, deep mixing substantially lowers the effective carbon flux J_{eff}, as compared to J_{exp}; low rain ratios at depth also contribute to a further decrease. In the context of the role of the biological pump in carbon sequestration it is, additionally, intuitively clear that small changes in depths of maximal mixing in the tropics will have a larger effect than corresponding changes at high latitudes.

The major features of Plate 1, depicting highest fluxes in regions of equatorial upwelling and at the continental margins, are similar to

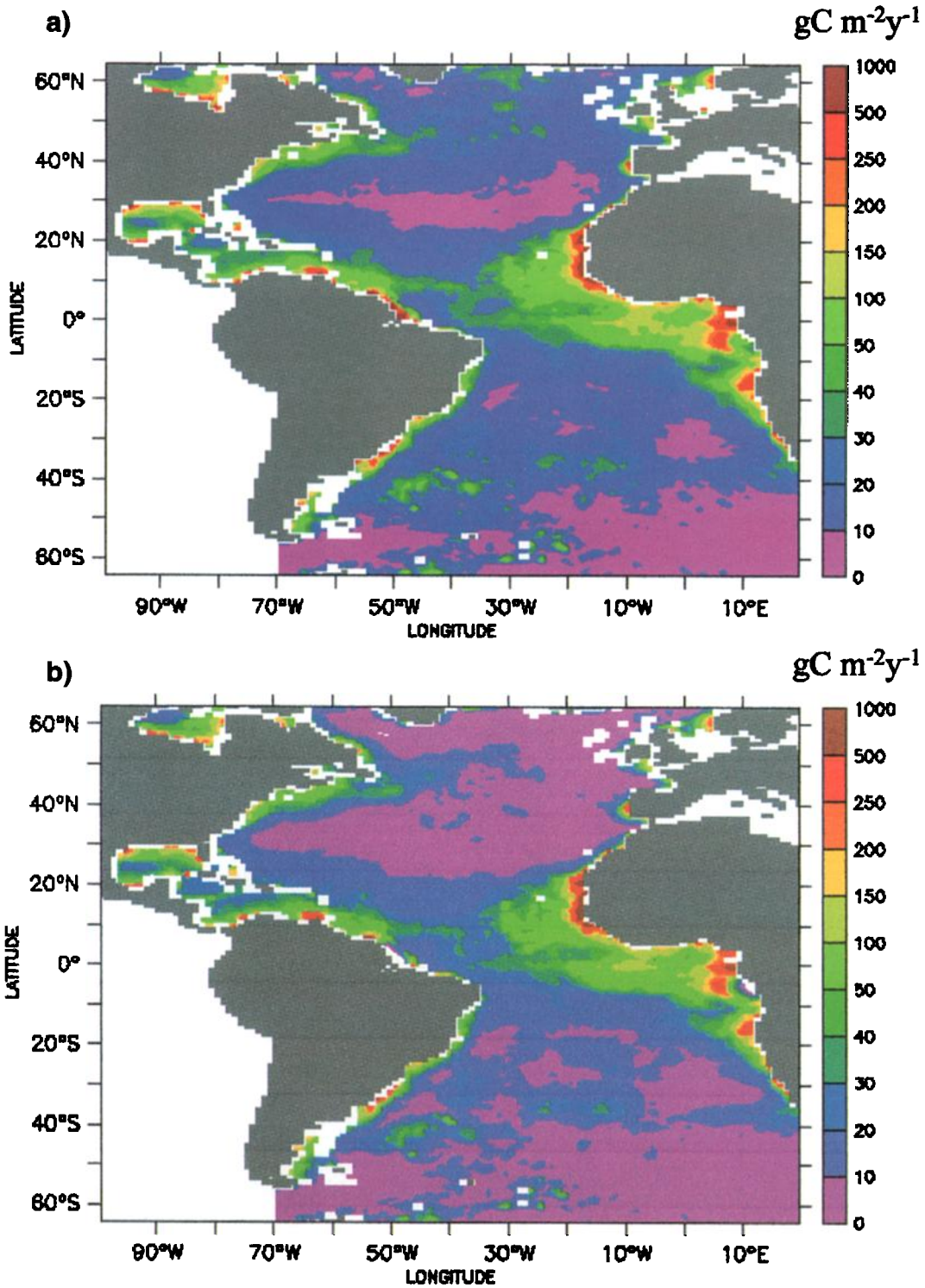

Plate 1. (a) J_{exp}, the export flux, as defined in text (J_{exp} = max (J_{125}, J_{WML})), where J_{125} and J_{WML} are the POC fluxes at 125 m and the winter mixed layer, respectively. (b) J_{eff}, the "effective carbon flux" at the base of the winter mixed layer, calculated as per equation (3) in text.

the patterns of benthic flux reported by *Jahnke* [1996]. Locally, and on shorter timescales, however, this pattern may vary considerably from the annual mean as a result of topographic effects on the seabed and the effects of short, rapid pulses of detrital input to the seabed. Remineralization above the winter mixed layer, $R_{EXP-WML}$, amounts to 0.19 Gt C yr^{-1}, or 5.7% of J_{exp}. This represents the fraction of export production that is not sequestered from contact with the atmosphere for climatically relevant timescales. This estimate is a minimal figure, since polar and subpolar regions, where winter mixing is deepest, are excluded from our analysis

A comparison of J_{eff} (Plate 1b) with primary production shows the importance of tropical upwelling regions, as a result of shallow winter mixed layers and high export fluxes (and f ratios). These regions make a large contribution to basin-wide export flux, whereas the spring bloom areas of the North Atlantic are of secondary importance. The effect of calcite fluxes on the effective carbon flux is greatest for the latitudinal bands north of 40°N and south of 30°S, where rain ratios of ~2 at the (deep) WML are significantly lower than rain ratios of 4–5.5 at the (shallow) WML depths in the oligotrophic equatorial Atlantic. This leads to a further enhancement of the tropical upwelling regions in basin-wide export and a further diminishing of the importance of the temperate bloom areas.

3.9. Feedbacks to Climate

As has been pointed out by *Smith and Mackenzie* [1991], the mere functioning of an oceanic biological pump is not sufficient to alter atmospheric CO_2 levels or to respond to anthropogenic CO_2 increase unless one of two conditions are met: a change in the efficiency of stripping available nutrients or an increase in availability and use of nutrients from land runoff. As discussed here, the effective carbon fluxes from the biological pump can vary as a function of changes in ventilation depth and rain ratio that are independent of these conditions. Projected changes in wind-driven mixing in the temperate North Atlantic, aside from altering nutrient availability and thus the absolute levels of export production, will change the efficiency of sequestration by the combined effect of shallower ventilation (and thus equilibration with the atmosphere) and the higher rain ratio. Additional changes due to a shift from opal- to carbonate-producing organisms will have a negative feedback, lowering sequestration efficiency.

4. Conclusions

1. Variable and unknown collection efficiencies of sediment traps are a major problem for the determination of export ratios. Future studies should routinely include an estimation of such efficiencies.
2. An empirical algorithm based on ^{230}Th-corrected data yields differences in export (f) ratio at 125 m of between 0.1 and 0.37 over a range of primary production between 50 and 400 g C m^{-2} yr^{-1}.
3. There are significant regional differences both in export at the base of the euphotic zone as well as the function describing POC degradation with depth. These reflect regional differences in flux seasonality and composition of sedimenting particles.
4. Interannual variations in primary production, for which data are available for only one station, show corresponding differences in annual POC flux.
5. Large differences in shallow fluxes are not apparent below 3000 m, indicating that there are significant and important differences in the biogeochemistry of the mesopelagic zone.
6. Effective carbon flux, defined as that flux causing a potential sequestration of CO_2 from the atmosphere, is calculated using organic carbon fluxes and rain ratios (POC:PIC) at the base of the winter mixed layer.
7. Tropical upwelling regions are potentially major sequestration centers of carbon due to the combined effect of shallow winter ventilation and high rain ratios at the winter mixed layer.
8. Of the export flux at the base of the euphotic zone, 5.7% is remineralized above the winter mixed layer between 65°N and 65°S.

Acknowledgments. We thank Aloys Bory for providing us data from the EUMELI site in digital form and Andreas Oschlies for providing new production estimates. We are grateful to Hugh Ducklow and two anonymous referees whose comments contributed to improvements in the manuscript. The time series data that go into this analysis were collected by a large number of unnamed people over many years; without their continued and dedicated work, a synopsis of the kind presented here would not have been possible. The Ocean Flux Program time series has been supported by the U.S. National Science Foundation since its inception. This publication is part of the German JGOFS Synopsis funded by the Bundesminister für Bildung, Forschung und Technologie (Bmb + f) and the Deutsche Forschungsgemeinschaft (DFG).

References

Altabet, M. A., Particulate new nitrogen fluxes in the Sargasso Sea, *J. Geophys. Res., 94*, 12,771–12,779, 1989.

Antia, A. N., B. von Bodungen, and R. Peinert, Particle Flux across the mid-European continental margin, *Deep Sea Res., Part I, 46*, 1999–2024, 1999.

Antoine, D., J.-M. Andre, and A. Morel, Oceanic primary production, 2, Estimation at global scale from satellite (coastal zone color scanner) chlorophyll, *Global Biogeochem. Cycles, 10*, 57–69, 1996.

Archer, D., and E. Meier-Reimer, Effect of deep-sea sedimentary calcite preservation on atmospheric CO_2 concentration, *Nature, 367*, 260–263, 1994.

Bacon, M. P., C. A. Huh, A. P. Fleer, and W. Deuser, Seasonality in the flux of natural radionuclides and plutonium in the deep Sargasso Sea, *Deep Sea Res., Part A, 32*, 273–286, 1985.

Bauerfeind, E., C. Garrity, M. Krumbholz, R. O. Ramseier, and M. Voss, Seasonal variability of sediment trap collections in the Northeast Water Polynia, part 2, Biochemical and microscopic composition of sedimenting matter, *J. Mar. Syst., 10*, 371–389, 1997.

Behrenfeld, M. J., and P. G. Falkowski, Photosynthetic rates derived from satellite-based chlorophyll concentration, *Limnol. Oceanogr., 42*, 1–20, 1997.

Berger, W. H., and G. Wefer, Export production: Seasonality and intermittency, and paleoceanographic implications, *Paloegeogr. Paleoclimatol. Paleoecol., 89*, 245–254, 1990.

Berger, W. H., K. Fischer, C. Lai, and G. Wu, Ocean carbon flux: Global maps of primary production and export production, in *Biogeochemical Cycling and Fluxes Between the Deep Euphotic Zone and Other Oceanic Realms*, edited by C. Agegian, *SIO Ref. 87-30*, pp. 1–44, Univ. of Calif., San Diego, Scripp Inst. of Oceanogr., La Jolla, Calif., 1987.

Betzer, P. R., W. J. Showers, E. A. Laws, C. D. Winn, G. R. DiTullio, and P. M. Kroopnick, Primary productivity and particle fluxes on a transect of the equator at 153°W in the Pacific Ocean, *Deep Sea Res., Part A, 31*, 1–11, 1984.

Bory, A. J.-M., and P. P. Newton, Transport of airborne lithogenic material down through the water column in two contrasting regions of the eastern subtropical North Atlantic Ocean, *Global Biogeochem. Cycles, 14*, 297–315, 2000.

Boyd, P. W., and P. P. Newton, Does planktonic community structure determine downward particulate organic carbon flux in different oceanic provinces?, *Deep Sea Res., Part I, 46*, 63–91, 1999.

Buesseler, K. O., Do upper-ocean sediment traps provide an accurate record of the particle flux?, *Nature, 353*, 420–423, 1991.

Buesseler, K. O., D. K. Steinberg, A. F. Michaels, R. J. Johnson, J. E. Andrews, J. R. Valdes, and J. F. Price, A comparison of the quantity and composition of material caught in a neutrally buoyant versus surface-tethered sediment trap, *Deep Sea Res., Part I, 47*, 277–294, 2000.

Campbell, J. W., and T. Aarup, New production in the North Atlantic derived from seasonal patterns of surface chlorophyll, *Deep Sea Res., Part A, 39*, 1669–1694, 1992.

Conte, M. H., N. Ralph, and E. H. Ross, Seasonal and interannual variability in deep ocean particle fluxes at the Ocean Flux Program (OFP) (Bermuda Atlantic Time Series (BATS)) site in the western Sargasso Sea near Bermuda, *Deep Sea Res., Part II, 48*, 1471–1505, 2001.

Deuser, W. G., Seasonal and interannual variations in deep-water particle fluxes in the Sargasso Sea and their relation to surface hydrography, *Deep Sea Res., Part A, 33*, 225–246, 1986.

Deuser, W. G., Temporal variability of particle flux in the deep Sargasso Sea, in *Particle Flux in the Ocean*, edited by V. Ittekot et al., pp. 185–198, John Wiley, New York, 1996.

Deuser, W. G., T. D. Jickells, P. King, and J. A. Commeau, Decadal and annual changes in biogenic opal and carbonate fluxes to the deep Sargasso Sea, *Deep Sea Res., Part I, 42*, 1923–1995, 1995.

Dugdale, R. C., and J. J. Goering, Uptake of new and regenerated forms of nitrogen in primary productivity, *Limnol. Oceanogr., 12*, 196–206, 1967.

Dugdale, R. C., F. P. Wilkerson, R. T. Barber, and F. P. Chavez, Estimating

new production in the equatorial Pacific Ocean at 150°W, *J. Geophys. Res.*, *97*, 681–686, 1992.

Eppley, R. W., and B. J. Peterson, Particulate organic matter flux and planktonic new production in the deep ocean, *Nature*, *282*, 677–680, 1979.

Eppley, R. W., E. H. Renger, andP. R. Betzer, The residence time of particulate organic carbon in the surface layer of the ocean, *Deep Sea Res.*, *30*, 311–323, 1983.

Falkowski, P. G., R. T. Barber, and V. Smetacek, Biogeochemical controls and feedbacks on ocean primary production, *Science*, *281*, 200–206, 1998.

Fischer, G., V. Ratmeyer, and G. Wefer, Organic carbon fluxes in the Atlantic and the Southern Ocean: Relationship to primary production compiled from satellite radiometer data, *Deep Sea Res., Part II*, *47*, 1961–1997, 2000.

Frankignoulle, M., C. Canon, and J.-P. Gattuso, Marine calcification as a source of carbon dioxide: Positive feedback of increasing atmospheric CO_2, *Limnol. Oceanogr.*, *39*, 458–462, 1994.

Gust, G., A. F. Michaels, R. Johnson, W. G. Deuser, and W. Bowles, Mooring line motions and sediment trap hydromechanics: In situ intercomparison of three common deployment designs, *Deep Sea Res., Part I*, *41*, 831–857, 1994.

Hebbeln, D., Flux of ice-rafted detritus from sea ice in the Fram Strait, *Deep Sea Res., Part II*, *47*, 1773–1790, 2000.

Hebbeln, D., and G. Wefer, Effects of ice coverage and ice-rafted material on sedimentation in the Fram Strait, *Nature*, *350*, 409–411, 1991.

Honjo, S., and S. J. Manganini, Annual biogenic particle fluxes to the interior of the North Atlantic Ocean studied at 34°N, 21°W and 48°N, 21°W, *Deep Sea Res., Part I*, *40*, 587–607, 1993.

Honjo, S., S. J. Manganini, and G. Wefer, Annual particle flux and a winter outburst of sedimentation in the northern Norwegian Sea, *Deep Sea Res., Part A*, *35*, 1223–1234, 1988.

Jackson, J. E., *A User's Guide to Principal Components*, 569 pp., John Wiley, New York, 1991.

Jahnke, R., The global ocean flux of particulate organic carbon: Areal distribution and magnitude, *Global Biogeochem. Cycles*, *10*, 71–88, 1996.

Jenkins, W. J., Nitrate flux into the euphotic zone near Bermuda, *Nature*, *331*, 521–523, 1988.

Kähler, P., and E. Bauerfeind, Organic particles in a shallow sediment trap: Substantial losses to the dissolved phase, *Limnol. Oceanogr.*, *46*, 719–723, 2001.

Kano, J., Relation between increase of coral and atmospheric carbon dioxide concentration, *Sora*, *65*, 1–7, 1990.

Karl, D., R. Letelier, L. Tupas, J. Dore, J. Christian, and D. Hebel, The role of nitrogen fixation in biogeochemical cycling in the subtropical North Pacific Ocean, *Nature*, *388*, 533–538, 1997.

Kuss, J., and K. Kremling, Particulate trace elemental fluxes in the deep north-east Atlantic Ocean, *Deep Sea Res., Part I*, *46*, 149–169, 1999.

Lampitt, R., Evidence for the seasonal deposition of detritus to the deep-sea floor and its subsequent resuspension, *Deep Sea Res., Part A*, *32*, 885–897, 1985.

Lampitt, R. S., and A. N. Antia, Particle flux in deep seas: Regional characteristics and temporal variability, *Deep Sea Res., Part I*, *44*, 1377–1403, 1997.

Lande, R., and A. M. Wood, Suspension times of particles in the upper ocean, *Deep Sea Res., Part A*, *34*, 61–72, 1987.

Lohrenz, S. E., G. A. Knauer, V. L. Asper, M. Tuel, A. F. Michaels, and A. H. Knap, Seasonal variability in primary production and particle flux in the northwestern Sargasso Sea: U.S. JGOFS Bermuda Atlantic Time-series Study, *Deep Sea Res., Part A*, *39*, 1373–1391, 1992.

Longhurst, A., *Ecological Geography of the Sea*, 398 pp., Academic, San Diego, Calif., 1998.

Longhurst, A., S. Sathyedranath, T. Platt, and C. Caverhill, An estimate of global primary production in the ocean from satellite radiometer data, *J. Plankton Res.*, *17*, 1245–1271, 1995.

Michaels, A. F., and A. H. Knap, Overview of the U.S. JGOFS Bermuda Atlantic Time-series Study and the Hydrostation S program, *Deep Sea Res., Part II*, *43*, 157–198, 1996.

Michaels, A. F., A. H. Knap, R. L. Dow, K. Gundersen, R. J. Johnson, J. Sorensen, A. Close, G. A. Knauer, S. E. Lohrenz, and V. A. Asper, Seasonal patterns of ocean biogeochemistry at the U.S. JGOFS Bermuda Atlantic Time-series Study Site, *Deep Sea Res., Part I*, *41*, 1013–1038, 1994.

Milliman, J. D., P. J. Troy, W. M. Balch, A. K. Adams, Y. H. Li, and F. T. Mackenzie, Biologically mediated dissolution of calcium carbonate above the chemical lysocline?, *Deep Sea Res., Part I*, *46*, 1653–1669, 1999.

Monterey, G., and S. Levitus, Seasonal variability of mixed layer depth for the world ocean, *NOAA Atlas NESDIS 14*, 96 pp., U.S. Govt. Print. Off., Washington, D.C., 1997.

Mortlock, R. D., and P. N. Fröhlich, A simple method for the rapid determination of biogenic opal in pelagic marine sediments, *Deep Sea Res., Part A*, *36*, 1415–1426, 1989.

Najjar, R. G., and R. F. Keeling, Mean annual air-sea oxygen flux: A global view, *Global Biogeochem. Cycles*, *14*, 573–584, 2000.

Neuer, S., V. Ratmeyer, R. Davenport, G. Fischer, and G. Wefer, Deep water particle flux in the Canary Island region: Seasonal trends in relation to long-term satellite derived pigment data and lateral sources, *Deep Sea Res., Part I*, *44*, 1451–1466, 1997.

Newton, P. P., R. S. Lampitt, T. D. Jickells, P. King, and C. Boutle, Temporal and spatial variability of biogenic particle fluxes during the JGOFS northeast Atlantic process studies at 47°N 20°W, *Deep Sea Res., Part I*, *41*, 1617–1642, 1994.

Noji, T. T., K. Y. Borsheim, F. Rey, and R. Norvedt, Dissolved organic carbon associated with sinking particles can be crucial for estimates of vertical carbon flux, *Sarsia*, *84*, 129–135, 1999.

Oschlies, A., and V. Garcon, Eddy-induced enhancement of primary production in a model of the North Atlantic Ocean, *Nature*, *394*, 266–269, 1998.

Pace, M. L., G. A. Knauer, D. M. Karl, and J. H. Martin, Primary production, new production and vertical flux in the eastern Pacific, *Nature*, *325*, 803–804, 1987.

Peinert, R., A. N. Antia, E. Bauerfeind, O. Haupt, M. Krumbholz, I. Peeken, B. von Bodungen, R. Ramseier, M. Voss, and B. Zeitzschel, Particle flux variability in the polar and Atlantic biogeochemical provinces of the Nordic seas, in *The Northern North Atlantic: A Changing Environment*, edited by P. Schäfer et al., pp. 53–68, Springer-Verlag, New York, 2001.

Rey, F., Development of the spring phytoplankton outburst at selected sites off the Norwegian coast, in *The Norwegian Coastal Current*, edited by R. Saetre and M. Mork, *2*, pp. 649–680, 1991.

Riebesell, U., I. Zondervan, B. Rost, P. D. Tortell, R. E. Zeebe, and F. Morel, Reduced calcification of marine plankton in response to increased atmospheric CO_2, *Nature*, *407*, 364–367, 2000.

Sarnthein, M., U. Pflaumann, R. Ross, R. Tiedemann and K. Winn, Transfer functions to reconstruct ocean paleoproductivity: A comparison, in *Upwelling Systems: Evolution Since the early Miocene*, edited by C. P. Summerhayes, W. L. Prell, and K. C. Emeis, *Geol. Soc. Spec. Publ.*, *64*, 411–427, 1992.

Schlitzer, R., Applying the adjoint method for biogeochemical modelling, in *Inverse Methods in Global Biogeochemical Cycles, Geophys. Monogr. Ser.*, vol. 114, edited by P. Kasibhatla et al., pp 107–124, AGU, Washington, D. C., 2000.

Schlüter, M., E. J. Sauter, A. Schäfer, and W. Ritzrau, Spatial budget of organic carbon flux to the seafloor of the northern North Atlantic (60°N–80°N), *Global Biogeochem. Cycles*, *14*, 329–340, 2000.

Scholten, J. C., F. Fietzke, S. Vogler, M. Rutgers van der Loeff, A. Mangini, W. Koeve, J. Waniek, P. Stoffers, A. Antia, and J. Kuss, Trapping efficiency of sediment traps from the deep eastern North Atlantic: ^{230}Th calibration, *Deep Sea Res., Part II*, *48*, 243–268, 2001.

Siegel, D. A., and W. G. Deuser, Trajectories of sinking particles in the Sargasso Sea: Modelling of "statistical funnels" above deep-ocean sediment traps, *Deep Sea Res., Part I*, *44*, 1519–1541, 1997.

Smith, S. V., and F. T. Mackenzie, Comments on the role of oceanic biota as a sink for anthropogenic CO_2, *Global Biogeochem. Cycles*, *5*, 189–190, 1991.

Steinberg, D. K., C. A. Carlson, N. R. Bates, R. J. Johnson, A. F. Michaels, and A. H. Knap, Overview of the US JGOFS Bermuda Atlantic Time-series Study (BATS): A decade look at ocean biology and biogeochemistry, *Deep Sea Res., Part II*, *48*, 1405–1447, 2001.

Suess, E., Particulate organic carbon flux in the oceans-surface productivity and oxygen utilisation, *Nature*, *288*, 260–263, 1980.

Tsunogai, S., and S. Noriki, Particulate fluxes of carbonate and organic carbon in the ocean: Is the marine biological activity working as a sink of the atmospheric carbon?, *Tellus, Ser. A*, *43*, 256–266, 1991.

von Bodungen, B., A. N. Antia, E. Bauerfeind, O. Haupt, I. Peeken, R. Peinert, S. Reitmeier, C. Thomsen, M. Voss, M. Wunsch, U. Zeller, and B. Zeitzschel, Pelagic processes and vertical flux of particles: An overview over a long-term comparative study in the Norwegian Sea and Greenland Sea, *Geol. Rundsch.*, *84*, 11–27, 1995.

Waniek, J., W. Koeve, and R. S. Prien, Trajectories of sinking particles and the catchment areas in the north east Atlantic, *J. Mar. Res.*, *58*, 983–1006, 2000.

Wassmann, P., Retention versus export food chains: Processes controlling

sinking loss from marine pelagic systems, *Hydrobiologia*, *363*, 29–57, 1998.

Wefer, G., and G. Fischer, Annual primary production and export flux in the Southern Ocean from sediment trap data, *Mar. Chem.*, *35*, 597–613, 1991.

Wefer, G., and G. Fischer, Seasonal patterns of vertical particle flux in equatorial and coastal upwelling areas of the eastern Atlantic, *Deep Sea Res., Part I*, *40*, 1613–1645, 1993.

Wefer, G., W. H. Berger, J. Bijma, and G. Fischer, Clues to ocean history: A brief overview of proxies, in *Use of Proxies in Paeoceanography: Examples From the South Atlantic*, edited by G. Fischer and G. Wefer, pp. 1–68, Springer-Verlag, New York, 1999.

A. N. Antia, U. Fehner, W. Koeve, K. Kremling, R. Peinert, and B. Zeitzschel, Institut für Meereskunde, Forschungsbereich Biogeochemie, Düsternbrooker Weg 20, D-24145 Kiel, Germany. (aantia@ifm.uni-kiel.de; w.koeve@sciencenet.com; kkremling@ifm.uni-kiel.de; rpeinert@sfb313.uni-kiel.de)

U. Bathmann, Alfred Wegener Institut für Polarforschung, Am Handelshaven 12, D-27570 Bremerhaven, Germany. (ubathmann@awi-bremerhaven.de)

T. Blanz J. Kuss, and D. Schulz-Bull, Insitut für Ostseeforschung-Warnemünde, Seestrasse 15, D-18119 Warnemünde, Germany. (thomas.blanz@io-warnemuende.de; detlef.schulz-bull@io-warnemuende.de)

M. Conte, Woods Hole Oceanographic Institution, 266 Woods Hole Road, Woods Hole, MA 02540, USA. (mconte@whoi.edu)

G. Fischer and D. Hebbeln, Fachbereich Geowissenschaften, Universität Bremen, Klagenfurter Strasse, D-28359 Bremen, Germany. (g05f@zfn.uni-bremen.de; dhebbeln@uni-bremen.de)

S. Neuer, Department of Biology, Arizona State University, Tempe, AZ 85287-1501, USA. (susanne.neuer@asu.edu)

J. Scholten, Geologisches Institut, Universität Kiel, Olsenhauerstr. 40-60, D-24118 Kiel, Germany. (js@gpi.uni-kiel.de)

(Received November 30, 2000; revised May 3, 2001;
accepted June 26, 2001.)